ACS EARTH AND SPACE CHEMISTRY

Article

Cite This: ACS Earth Space Chem. 2019, 3, 2339−2352

http://pubs.acs.org/journal/aesccq

Characterization of Secondary Organic Aerosol Tracers over Tianjin, North China during Summer to Autumn

Yu Wang,[†] Chandra Mouli Pavuluri,[*,†] Pingqing Fu,[†] Peisen Li,[†] Zhichao Dong,[†] Zhanjie Xu,[†] Hong Ren,[†] Yanbing Fan,[†] Linjie Li,[‡] Yan-Lin Zhang,[§] and Cong-Qiang Liu[†]

[†]Institute of Surface-Earth System Science, Tianjin University, Tianjin 300072, China

[‡]LAPC, Institute of Atmospheric Physics, Chinese Academy of Sciences, Beijing 100029, China

[§]Yale-NUIST Center on Atmospheric Environment, Nanjing University of Information Science and Technology, Nanjing 10044, China

Supporting Information

ABSTRACT: To characterize secondary organic aerosols (SOA) over the Tianjin region, we studied the SOA tracers derived from isoprene, α/β-pinene, β-caryophyllene, and aromatics in $PM_{2.5}$ collected at an urban site and a background site over Tianjin, North China during summer to autumn 2018. Concentrations of total isoprene SOA tracers were twice those of α/β-pinene in summer, while they were the opposite in autumn, followed by β-caryophyllinic acid and 2,3-dihydroxy-4-oxopentanoic acid (2,3-DHOPA), the only tracers derived from β-caryophyllene and toluene, respectively. The isoprene and α/β-pinene SOA tracers were abundant in summer, whereas β-caryophylinic acid and 2,3-DHOPA dominated in autumn. Temporal variations and linear relations of SOA tracers with ambient temperature and molecular markers (levoglucosan and hopanes) together with the air mass trajectories implied that the SOA derived from terrestrial vegetation and marine biota and biomass burning was high in summer and autumn, respectively, while that derived from fossil fuel combustion and its processing during long-range atmospheric transport were significant in both seasons. The estimated SOA derived from aromatics was found to be most abundant, followed by that from sesquiterpenes, monoterpenes, and isoprene, respectively. The contribution of total SOC to OC and WSOC varied between 4.16% and 23.7% and 6.28−30.7%, respectively, in which biogenic SOC accounted for about 50% in summer and 40% in autumn, indicating significant loading of SOA over Tianjin, North China.

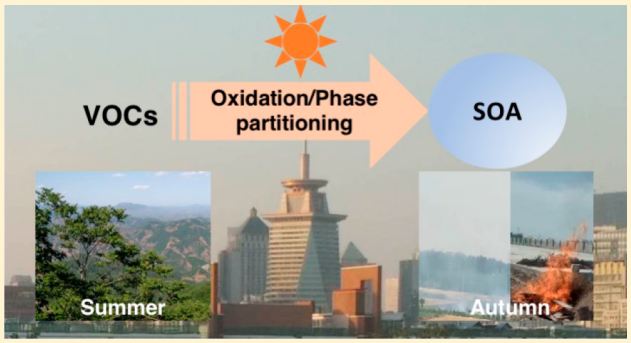

KEYWORDS: *Secondary organic aerosols, biogenic emissions, biomass burning, long-range atmospheric transport, North China*

INTRODUCTION

Organic aerosols (OA) account for a significant fraction (20−50%) in midlatitudes and an even dominant fraction (up to 90%) in forested areas.[1] They have a severe impact on the Earth's climate system directly by absorbing and scattering solar radiation and indirectly by acting as cloud condensation nuclei (CCN).[2] OA can also adversely affect human health[3,4] and play an important role in atmospheric chemistry.[5] They are emitted directly from natural and anthropogenic sources such as fossil fuel combustion, biomass burning, soil suspension, biological species, and agricultural waste (primary, POA) and formed by reactions of volatile organic compounds (VOCs) that are emitted from a variety of sources including vegetation, biomass burning, and fossil fuel combustion with O_3, OH, and NO_3 radicals and subsequent nucleation and/or condensation onto pre-existing aerosols of the resulted low-volatility compounds in the atmosphere (secondary, SOA).[6−10] SOA accounts for ∼60% of OA globally and even more on a regional scale.[1] Vegetation releases large amounts of VOCs, including isoprene, monoterpenes, sesquiterpenes, and oxygenated hydrocarbons.[11,12] On a global scale, biogenic VOCs were estimated to be 1150 TG yr^{-1} with a predominance of isoprene (44%) followed by monoterpenes (11%),[11] whereas anthropogenic VOCs were only 110 Tg yr^{-1}, in which aromatics account for 13%.[13] Thus, the SOA formed from biogenic emissions is believed to be larger than that from anthropogenic sources.[1] However, the contribution of SOA from anthropogenic sources often exceeds 50% in most populated regions, including Asia, due to human activities.[14] Besides, the anthropogenic emissions in urban localities might accelerate the oxidation of BVOCs and enhance the SOA formation.[15,16]

Received: June 12, 2019
Revised: August 14, 2019
Accepted: August 22, 2019
Published: August 22, 2019

DOI: 10.1021/acsearthspacechem.9b00170
ACS Earth Space Chem. 2019, 3, 2339−2352

Specific molecular marker compounds (tracers) could provide insights into the origins of OA and precursors of SOA as well as its formation processes that influence SOA evolution and spatiotemporal distribution in the atmosphere. Isoprene-derived SOA (SOA_I) has been regarded as negligible due to the high volatility of its known reaction products and the low SOA yield,[17] despite its large flux.[12] However, identification of two diastereoisomeric 2-methyltetrols in Amazonian rain forest aerosols as isoprene oxidation products by Claeys et al.[18] has changed the way the scientific community thinks of SOA_I. Furthermore, the discovery of isoprene epoxydiols (IEPOX) formation by reactions of isoprene with OH and HO_2 radicals (HO_2-channel)[19−21] under low-NO_x (NO_x = NO + NO_2) conditions, and 2-methylglyceric acid (2-MGA) and methacrylic acid epoxide (MAE) by reactions with NO and NO_2 radicals (NO_x-channel)[22,23] under high-NO_x conditions, and the influence of aerosol acidity[24] and relative humidity[23] on their yield, has expanded the understanding of the formation processes of SOA_I. Currently, isoprene is believed to be a large biogenic source of SOA loading, and the contribution of SOA_I is estimated to be 2−19.2 Tg yr^{-1} on the global scale,[18,25] accounting for about 70% of the total SOA.[26]

Monoterpene- (SOA_M) and sesquiterpene-derived SOA (SOA_S) are also considered significant contributors to SOA loading in the atmosphere. Previous experiments on monoterpene oxidation under natural or artificial sunlight found the product species with either endocyclic double bonds (in the case of α-pinene) or exocyclic double bonds (in the case of β-pinene), which lead to the understanding of SOA_M formation processes.[27] It has been established that *cis*-pinonic acid (PNA) and pinic acid (PA) are the first-generation major products formed by the reaction of α- and β-pinene with O_3[28] and OH radicals.[29] PNA and PA can be further photooxidized to high-generation products such as 3-methyl-1,2,3-butanetricarboxylic acid (3-MBTCA).[30] Moreover, it has been found that highly oxygenated products such as 3-hydroxyglutaric acid (3-HGA) are formed by photooxidation of α-pinene in the presence of NO_x through reactions that involve O_3 and OH radicals.[31] β-Caryophyllinic acid (β-CPA) has been identified as a specific tracer for SOA_S.[32] The amount of biogenic SOA is estimated to be in the range of 9−50 Tg yr^{-1} using global bottom-up models,[1] and up as high as 185 Tg yr^{-1} by top-down models.[33] Also, 2,3-dihydroxy-4-pentanoic acid (2,3-DHOPA) has been found to be produced by photooxidation of toluene and is considered a tracer for SOA derived from anthropogenic aromatics (SOA_A),[34,35] and the contribution of SOA_A is reported to be highly significant and even larger than that of biogenic SOA in some locations.[35,36]

Kleindienst et al.[35] estimated the contributions of biogenic SOA as well as anthropogenic SOA using the mass fractions of the tracers obtained from photochemical oxidation of isoprene, α-pinene, and β-caryophyllene and toluene in chamber experiments. Furthermore, the SOA tracers have been reported in ambient aerosols from forested or mountain[18,35,37−42] and urban areas[15,36,43−45] as well as the Arctic region,[46] which provides insights on SOA formation and transformation processes and its loading at those locales. Atmospheric aerosol loading is commonly observed to be high in East Asia. China is the largest developing country in this region, and its economy has been growing at a very rapid rate over the past decades. Currently, fine ($PM_{2.5}$) aerosol concentrations exceed the national air quality standards in most cities[47] and have become a serious environmental problem in China. In fact, the contribution of SOA to $PM_{2.5}$ and OA has been estimated to be up to 35% and 71%, respectively,[48] and thus, SOA plays an important role in deteriorating the air quality in China. Previous modeling studies predicted that biogenic VOCs are the major contributors of SOA in China[49,50] but ground-based observation studies, particularly in North China, suggest that anthropogenic aromatics are the largest SOA contributors.[36,51]

Studies on biogenic and anthropogenic SOA tracers and their formation processes and loading are very limited in North China,[15,36,51,52] particularly in the Tianjin−Hebei region, where high aerosol loading is prevalent and often suffers from haze events,[53,54] and where the air quality is poor.[55] Tianjin is one of the fastest developing regions in China, and hence, the anthropogenic pollutant emissions are very high. However, the Tianjin region is covered with rich vegetation, including agricultural lands and forests. In addition, Tianjin is located adjacent to Bohai sea, and hence, the impact of marine biogenic emissions on Tianjin aerosols is significant. Therefore, the potential for VOC emissions from biogenic and anthropogenic sources, including biomass burning, is high in this region, and thus, the formation of SOA is also high. Consequently, it is highly necessary to investigate the organic molecular composition of SOA tracers in Tianjin aerosols.

In this study, we aim to characterize the chemical composition and abundances of isoprene-, α/β-pinene-, β-caryophyllene-, and toluene-derived SOA tracers in atmospheric fine ($PM_{2.5}$) aerosols collected at an urban and a background site over Tianjin, North China during summer to autumn 2018. Also, we intend to estimate the contributions of secondary organic carbon (SOC) derived from biogenic and anthropogenic VOCs to organic carbon (OC) and water-soluble OC (WSOC) in the $PM_{2.5}$. The results will be discussed in terms of SOA origins, formation processes, and loading over Tianjin, and thus, this study provides a baseline data of SOA that will help to improve model simulations.

■ EXPERIMENTAL SECTION

Sample Collection. $PM_{2.5}$ samples were collected simultaneously at an urban site (Nankai district (ND) located at 39.11°N, 117.18°E) and a background site (Haihe Education Park (HEP) at 39.00°N, 117.32°E), which are 23 km away from each other in Tianjin (see Figure S1 in the Supporting Information), located on the lower reaches of Haihe River and adjacent to Bohai Sea with a population of ∼15 million (https://citypopulation.de/php/china-tianjin-admin.php). Coal is the main source of energy, and the industrial terminal energy consumption accounts for ∼66% of the total energy consumption. Agricultural activity is high in northern parts of the Tianjin region, which is also covered with mountains and dense forests. Therefore, the influence of fossil fuel combustion emissions is high at ND, whereas biogenic and/or biomass burning emissions as well as sea breezes greatly influence HEP. The regional climate over Tianjin is strongly affected by the East Asian monsoon that influences the origins of the long-range transported air masses that arrive in Tianjin. The sampling was performed on the rooftop of a 7-story building at Tianjin University (TJU) Weijin Road campus (ND; n = 39) and a 6-story building in TJU Peiyang Park campus (HEP; n = 20) using precombusted (450 °C, 4 h) quartz fiber filters (Pall, 2500QAT-UP) and a high-volume air sampler (Tisch Environmental, TE-6070DX) for ∼72 h each sample during summer to autumn (5 July to 30 October)

DOI: 10.1021/acsearthspacechem.9b00170
ACS Earth Space Chem. 2019, 3, 2339−2352

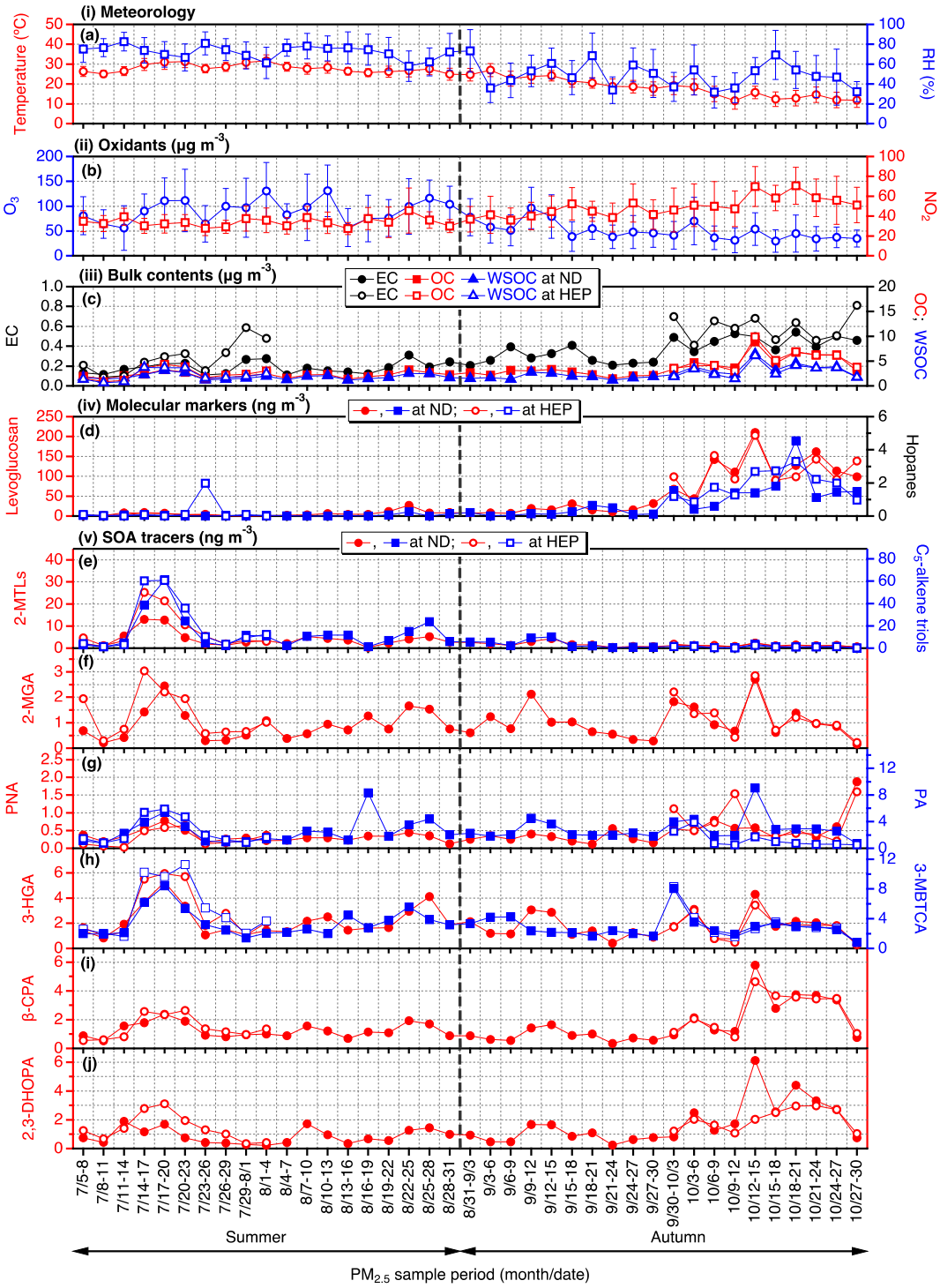

Figure 1. Temporal variations of (i) meteorological parameters, ambient temperature and relative humidity (RH) (a), and (ii) concentrations (μg m^{-3}) of oxidants O_3 and NO_2, (b) at Tianjin, and (iii) concentrations (μg m^{-3}) of bulk contents EC, OC, and WSOC (c) and (iv) those (ng m^{-3}) of molecular markers levoglucosan and hopanes ($\Sigma C_{27}-C_{32}$) (d), and (v) SOA_I (e,f), SOA_M (g,h), SOA_S (i), and SOA_A (j) tracers in $PM_{2.5}$ collected at an urban site (Nankai District, ND) and a background site (Haihe Education Park, HEP) in Tianjin during summer to autumn 2018. See text for abbreviations.

2018. The filter samples were placed in a precombusted glass jar with a Teflon-lined screw cap and stored at −20 °C in darkness prior to analysis. One blank filter sample was also collected in each season following the same procedure without the pump switched on.

Determination of Organic Tracers. $PM_{2.5}$ samples were extracted and derivatized following the procedure described elsewhere.[46] Briefly, filter aliquots were first extracted with 10 mL of dichloromethane/methanol (2:1; v/v, ANPEL Laboratory Technologies (Shanghai) Inc., 99.9%) for three times under ultrasonication for 10 min each. The extracts were filtered through quartz wool packed in a Pasteur pipet (ANPEL Laboratory Technologies (Shanghai) Inc.) and concentrated to about 100 μL under rotary evaporation and

DOI: 10.1021/acsearthspacechem.9b00170
ACS Earth Space Chem. 2019, 3, 2339−2352

then blown to dryness under pure nitrogen gas. The organic compounds were then reacted with 50 μL of *N*,*O*-bis-(trimethylsilyl)trifluoroacetamide (BSTFA) in the presence of 1% trimethylchlorosilane (Sigma-Aldrich) and 10 μL of pyridine (Sigma-Aldrich, 99.9%) at 70 °C for 3 h to derivatize the carboxyl group trimethylsilyl (TMS) esters and OH to TMS ethers. The derivatives were then diluted by adding 40 μL of *n*-hexane containing 1.43 ng μL^{-1} of an internal standard (C_{13} *n*-alkane, to determine the relative response) before injecting into a gas chromatograph/mass spectrometer (GC/MS, Hewlett-Packard 7890A GC coupled with 5975C MSD), equipped with a split/splitless injection and fused silica capillary column (DB-5MS, 30 m × 0.25 mm i.d., 0.25 μm film thickness). The derivatized samples were injected into the GC in a splitless mode at an injector temperature of 280 °C, and the compound separation was carried out on a capillary column with the GC oven temperature-programmed from 50 °C (2 min) to 120 °C (at 15 °C min^{-1}) and then to 300 °C (at 5 °C min^{-1}) with a final isothermal hold at 300 °C for 16 min. Helium was used as a carrier gas. The MS was operated in the electron ionization (EI) mode at 70 eV and scanned in the m/z range of 50 to 650 Da. Data were processed with Chemstation software.

Individual compounds of TMS derivatives of SOA tracers (and other marker species) were identified by comparison of mass spectra with those of authentic standards or literature data. PNA, PA, 3-HGA, and 2,3-DHOPA were quantified using their authentic standards, while the other SOA tracers were quantified using surrogate compounds: erythritol for 2-methyltetrols (2-MTLs), C_5-alkene triols, and 2-methylglyceric acid (2-MGA),[18] PNA for 3-MBTCA, and PA for β-CPA,[41] due to lack of standards. The method detection limits for erythritol, PNA, PA, 3-HGA, and 2,3-DHOPA were 0.03, 0.08, 0.13, 0.06, and 0.05 ng m^{-3}, respectively, with the used sample volume of 30.0 m^3. Recoveries for authentic standards or surrogates that were spiked on to precombusted quartz filters were found to be more than 80%. Based on duplicate sample analysis, the analytical error was generally less than 10%. Field blank filter samples were treated following the same procedures for quality assurance, and no target SOA tracers, except for 3-HGA, were detected. The 3-HGA only appeared in one summer filter blank, but its concentration was less than 1% of that in actual samples, and the data presented here was corrected for the blank but not for recoveries.

Measurements of OC, EC, and WSOC. OC and EC were measured using the Sunset Laboratory OC/EC Analyzer (Sunset Laboratory Inc., USA) following the Interagency Monitoring of Protected Visual Environments (IMPROVE) thermal/optical evaluation protocol[56] and assuming the carbonate carbon to be negligible.[57] Briefly, an aliquot of filter sample (1.5 cm^2) was punched and inserted into a quartz boat inside the thermal desorption chamber of the analyzer and then combusted with stepwise heating. The evolved CO_2 was measured directly by a nondispersive infrared (NDIR) detector system, and the transmittance of light through the filter punch was used for OC correction. WSOC was measured using a TOC analyzer (TOC-V_{csh}, Shimadzu, Japan) after extracting an aliquot of filter samples (14 mm disc in diameter) into 20 mL of organic free Milli Q water under ultrasonication for 20 min.[57] Based on duplicate sample analysis, the analytical uncertainty in all measurements was generally less than 5%. All the concentrations reported here were corrected for field blanks.

Estimation of SOC. The isoprene-, monoterpene-, sesquiterpene-, and aromatics-derived SOC was estimated using a tracer-based method proposed by Kleindienst et al.,[35] using the measured concentrations of tracers in $PM_{2.5}$ and the laboratory-derived tracer mass fraction (f_{SOC}) factors of 0.155 ± 0.039 for isoprene, 0.231 ± 0.111 for α-pinene, 0.023 ± 0.0046 for β-caryophyllene, and 0.0079 ± 0.0026 for toluene by the following equation:

$$f_{SOC} = \Sigma_i[\text{tracer}]/[\text{SOC}]$$

where Σ_i[tracer] is the sum of the concentrations of the selected suite of tracers for the same precursor in $\mu g\ m^{-3}$. This technique was developed using a series of chamber experiments conducted under relatively high NO_x (0.11−0.65 ppm) conditions. However, it has been reported that the f_{SOC} derived for isoprene (range 0.117−0.231, ave. 0.156) in the absence of NO_x[58] is similar to that obtained under high NO_x conditions, although the NO_x influence of the f_{SOC} for other VOCs is not clear. Furthermore, the concentration of NO_2 in Tianjin ranged from 0.014 to 0.37 ppm with an average of 0.022 ppm during the campaign period (see Figure 1b). Hence, we consider the tracer-based method highly applicable for this study.

It should also be noted that Kleindienst et al.[35] derived the f_{SOC} by using ketopinic acid as the surrogate for quantification of all the SOA tracers, whereas, as detailed earlier, the SOA tracers in this study were quantified using authentic standards, together with some surrogates that were further quantified by GC-FID. Such differences could result in some degree of uncertainty. Furthermore, three compounds including 2-MGA and two 2-MTLs were used as tracers for SOA_I estimation, and β-CPA and 2,3-DHOPA were used as tracers for SOA_S and SOA_A estimation, respectively, in this study, which are the same as those used in Kleindienst et al.[35] Although Kleindienst et al. reported nine tracers for SOA_M estimation, we used only four compounds such as 3-HGA, PNA, PA, and 3-MBTCA determined in this study. However, we consider that the uncertainties due to the differences in the tracers used for SOA estimation should be within the uncertainties raised by the tracer-based approach itself (22−54%) due to the standard deviation of f_{SOC} mentioned above.

■ RESULTS AND DISCUSSION

Meteorology, Oxidants, and Backward Air Mass Trajectories. Hourly averaged meteorological data of Tianjin available online were downloaded from https://darksky.net/forecast/39.1236,117.1981/si12/en, and the oxidants (O_3 and NO_2) data were downloaded at http://beijingair.sinaapp.com. Averaged ambient temperature and relative humidity (RH) as well as O_3 and NO_2 for each sample period during the campaign are presented in Figure 1a,b. The ambient temperature ranged from 25.0 to 31.6 °C with an average of 28.0 ± 2.12 °C in summer and 11.6−27.0 °C (average 18.2 ± 4.81 °C) in autumn, and the RH ranged from 58.0 to 82.7% (72.3 ± 6.59%) and 31.8−73.2% (49.4 ± 12.6%), respectively. While the wind speed varied between 2.14 to 5.15 m s^{-1} with an average of 3.17 ± 0.78 m s^{-1} in summer and 1.76−4.99 m s^{-1} (3.28 ± 0.92 m s^{-1}) in autumn. Concentrations of O_3 and NO_2 were 91.7 ± 22.9 and 34.0 ± 4.5 $\mu g\ m^{-3}$, respectively, in summer and 50.1 ± 18.1 and 49.4 ± 9.80 $\mu g\ m^{-3}$ in autumn.

Cluster analysis of the air masses situated at 500 m above ground level over Tianjin for one-month period each during

DOI: 10.1021/acsearthspacechem.9b00170
ACS Earth Space Chem. 2019, 3, 2339−2352

the campaign was conducted using the five-day backward air mass trajectories data obtained from NOAA HYSPLIT modeling system (https://www.ready.noaa.gov/HYSPLIT.php). The computed plots are provided in the SI (Figure S2). The results show that about 94% of the air masses that arrived in Tianjin in July originated from the sea of Japan, East China Sea and/or western North Pacific Ocean, whereas only 19.5% of the air masses originated from the East China Sea in August, and the rest of the air masses originated from Siberia, Mongolia or China mainland in summer (Figure S2a,b). In autumn, about 50% and 73% of the air masses originated from Siberia in September and October, respectively, and the rest originated from northern China mainland (Figure S2c,d).

Carbonaceous Components. A summary of concentrations of elemental carbon (EC), OC, and WSOC observed at ND and HEP in Tianjin, North China in summer and autumn is presented in Table 1. Their temporal variations during the campaign are depicted in Figure 1c. Concentrations of EC and OC ranged from 0.11 to 0.54 μgC m^{-3} with an average of 0.28 ± 0.13 and 1.37−8.89 μgC m^{-3} (average 3.01 ± 1.64 μgC m^{-3}) at ND (n = 39) and 0.09−0.81 μgC m^{-3} (0.44 ± 0.21 μgC m^{-3}) and 0.85−9.86 μgC m^{-3} (3.86 ± 2.20 μgC m^{-3}) at HEP (n = 20), respectively, during the campaign, while WSOC ranged between 1.14 and 6.47 μgC m^{-3} (2.27 ± 1.08 μgC m^{-3}) at ND and 0.66−6.11 μgC m^{-3} (2.62 ± 1.34 μgC m^{-3}) at HEP. The average relative abundance of WSOC in OC was found to be 78.0 ± 12.3% at ND and 72.1 ± 17.8% at HEP. Concentrations of EC, OC, and WSOC observed in summer at ND (Table 1) were found to be lower than those (0.59, 5.25, and 3.48 μg m^{-3} in daytime and 0.74, 4.62, and 2.63 μg m^{-3} in the nighttime, respectively) reported in $PM_{2.5}$ collected from the same site in July 2016.[59] This is consistent with the recent decreasing trend in aerosol loading over China.[60]

WSOC can be directly emitted from biomass burning[61] and also formed by oxidation of VOCs in the atmosphere.[62] The mass ratio of WSOC to OC has been considered a measure of photochemical processing (aging) during long-range atmospheric transport,[63] if the influence of biomass burning is insignificant. Interestingly, the average WSOC/OC found at ND in summer (Table 1) was higher than that (63%) reported in summer 2016 from the same site.[59] Such high abundance of WSOC should be due to either enhanced emission from biomass burning and/or secondary formation from VOCs. As can be seen from Figure 1d, concentrations of levoglucosan, an excellent marker for biomass burning,[64] were found to be extremely low at both sites in summer, which suggests that the contribution of OA (including WSOC) from biomass burning was not significant. However, the air masses that arrived in Tianjin during summer, particularly in July when the OC, WSOC, and SOA tracers peaked, mostly originated from the oceanic region (Figure S2a,b), which means they should have been enriched with marine biogenic emissions and subsequently aged during long-range atmospheric transport. Therefore, the enhanced WSOC/OC implies that the loading of SOA is increasing over China, despite a decrease in overall aerosol burden in recent years, probably due to the increased oxidation capacity of the atmosphere. It is likely because O_3 concentrations (about 30%) and the mass ratios of OC to EC over China, particularly in Beijing−Tianjin−Heibei (BTH) region, were reported to be increasing annually in recent times.[60,65]

Composition and Abundances of SOA Tracers. Molecular distributions of isoprene-, α/β-pinene-, β-caryophyllene-, and toluene-derived SOA tracers determined in $PM_{2.5}$ collected at ND (n = 39) and HEP (n = 20) over Tianjin are depicted in Figure 2. Six isoprene oxidation products including two 2-MTLs (2-methylthreitol and 2-methylerythritol), three C_5-alkene triols (*cis*-2-methyl-1,3,4-trihydroxy-1-butene, 3-methyl-2,3,4-trihydroxy-1-butene, and *trans*-2-methyl-1,3,4-trihydroxy-1-butene), and 2-MGA were identified in Tianjin $PM_{2.5}$ collected at both the sites. Concentrations of 2-methylerythritol were always higher by a factor of 2−3 than that of 2-methylthreitol at both the sites in Tianjin (Table 1). Averages of 2-methylthreitol and 2-methylerythritol were found to be 0.75 ± 0.68 and 2.03 ± 2.13 ng m^{-3} at ND (n = 39) and 1.16 ± 1.47 and 3.47 ± 5.41 ng m^{-3} at HEP (n = 20), respectively, during the campaign. Those of the sums of C_5-alkene triols were 7.76 ± 11.9 ng m^{-3} at ND and 10.6 ± 18.9 ng m^{-3} at HEP, with a high abundance of *trans*-2-methyl-1,3,4-trihydroxy-1-butene (5.37 ± 8.24 ng m^{-3} at ND and 7.33 ± 13.1 ng m^{-3} at HEP) followed by *cis*-2-methyl-1,3,4-trihydroxy-1-butene (1.57 ± 2.35 and 2.16 ± 3.80 ng m^{-3}) and 3-methyl-2,3,4-trihydroxy-1-butene (0.83 ± 1.25 and 1.12 ± 2.00 ng m^{-3}), respectively, at both the sites during the campaign, while the average of 2-MGA was 0.96 ± 0.61 ng m^{-3} at ND and 1.27 ± 0.83 ng m^{-3} at HEP.

Four α/β-pinene oxidation products, PNA, PA, 3-HGA, and 3-MBTCA, were detected. Averages of PNA and PA were found to be 0.41 ± 0.29 and 2.73 ± 1.81 ng m^{-3} at ND and 0.50 ± 0.45 and 1.92 ± 1.69 ng m^{-3} at HEP, respectively, during the campaign. While those of 3-HGA and 3-MBTCA were 1.93 ± 1.12 and 3.16 ± 1.67 ng m^{-3} at ND and 2.30 ± 1.67 and 4.23 ± 3.12 ng m^{-3} at HEP, respectively. The average abundance of the sum of isoprene-derived tracers (11.5 ± 14.8 ng m^{-3}) was found to be slightly higher than that (8.22 ± 3.83 ng m^{-3}) of α/β-pinene-derived tracers at ND, whereas at HEP, it was higher by a factor of ∼2 (16.5 ± 26.1 and 8.96 ± 6.23 ng m^{-3}, respectively) during the campaign. β-CPA, an oxidation product of β-caryophyllene, and 2,3-DHOPA, an oxidation product of toluene, ranged from 0.35 to 5.78 ng m^{-3} (1.49 ± 1.10 ng m^{-3}) and 0.23−6.11 ng m^{-3} (1.32 ± 1.20 ng m^{-3}) at ND and 0.56−4.65 ng m^{-3} (1.99 ± 1.23 ng m^{-3}) and 0.34−3.11 ng m^{-3} (1.72 ± 0.88 ng m^{-3}) at HEP, respectively, during the campaign.

It is noteworthy that all the biogenic SOA tracers, except PA, were found to be abundant at HEP as compared to ND during the campaign (Figure 2). It is likely because the emission of biogenic VOCs must be higher at HEP, where human activities are less and most of the area is covered with dense vegetation. Furthermore, such spatial distributions indicate that SOA loading over Tianjin must be significantly influenced by local emissions, in addition to the contribution from long-range transported air masses. Interestingly, in consistence with that of biogenic SOA tracers, the average concentration of 2,3-DHOPA, an anthropogenic aromatics-derived SOA tracer, was also found to be higher at HEP than that at ND (Figure 2), although its peak was at ND in autumn (Figure 1j). Such high abundance of 2,3-DHOPA at HEP suggests that oxidants (OH_x, O_3, and NO_x) that promote the SOA formation from both biogenic and anthropogenic VOCs loading should be higher at HEP. But it is unlikely, because the anthropogenic emissions including automobile exhaust in HEP must be lower than those in ND. Alternatively, the 2,3-DHOPA might be

DOI: 10.1021/acsearthspacechem.9b00170
ACS Earth Space Chem. 2019, 3, 2339−2352

Table 1. Summary of Concentrations of Bulk Contents, SOA Tracers, and Contributions of Their C Contents to OC and WSOC in $PM_{2.5}$ at ND and HEP over Tianjin, North China in Summer and Autumn 2018[a]

	ND								HEP							
	Summer (n = 19)				Autumn (n = 20)				Summer (n = 10)				Autumn (n = 10)			
	Concentration		Percent C in		Concentration		Percent C in		Concentration		Percent C in		Concentration		Percent C in	
Species	Range	Ave ± SD	OC	WSOC	Range	Ave ± SD	OC	WSOC	Range	Ave ± SD	OC	WSOC	Range	Ave ± SD	OC	WSOC
Bulk carbonaceous contents (μgC m^{-3})																
EC	0.11–0.31	0.18 ± 0.06			0.21–0.54	0.37 ± 0.11			0.09–0.59	0.28 ± 0.16			0.41–0.81	0.59 ± 0.13		
OC	1.37–3.25	2.16 ± 0.55			1.48–8.89	3.83 ± 1.91			0.85–4.34	2.44 ± 1.20			3.01–9.86	5.28 ± 2.07		
WSOC	1.14–3.12	1.85 ± 0.55	85.5		1.16–6.47	2.66 ± 1.31	70.8		0.66–3.73	2.16 ± 1.17	86.6		1.48–6.11	3.08 ± 1.41	57.6	
SOA Tracers (ng m^{-3})																
Isoprene-derived SOA tracers																
2-Methylthreitol	0.14–3.15	1.08 ± 0.82	0.02	0.02	0.11–1.05	0.43 ± 0.25	0.01	0.01	0.32–6.16	1.88 ± 1.84	0.03	0.03	0.22–0.83	0.45 ± 0.18	0.004	0.01
2-Methylerythetol	0.15–9.89	3.05 ± 2.62	0.06	0.07	0.26–3.28	1.06 ± 0.74	0.01	0.02	0.81–19.2	6.16 ± 6.75	0.10	0.11	0.38–1.48	0.79 ± 0.33	0.01	0.01
Σ2-MTLs	0.29–13.0	4.13 ± 3.43	0.08	0.09	0.39–4.33	1.49 ± 0.98	0.02	0.03	1.13–25.3	8.05 ± 8.54	0.13	0.14	0.61–2.31	1.23 ± 0.51	0.01	0.02
cis-2-MTHB	0.22–12.1	2.65 ± 2.99	0.06	0.06	0.03–2.03	0.54 ± 0.57	0.01	0.01	0.30–12.3	4.08 ± 4.73	0.07	0.07	0.06–0.56	0.24 ± 0.15	0.002	0.004
3-MTHB	0.10–6.43	1.42 ± 1.58	0.03	0.03	0.01–1.07	0.27 ± 0.30	0.00	0.01	0.14–6.49	2.12 ± 2.49	0.03	0.04	0.03–0.25	0.12 ± 0.06	0.001	0.002
trans-2-MTHB	0.70–42.7	9.16 ± 10.5	0.19	0.22	0.06–7.00	1.76 ± 1.98	0.03	0.04	0.93–42.3	13.9 ± 16.2	0.22	0.25	0.15–1.69	0.74 ± 0.47	0.01	0.01
ΣC_5–Alkene triols	1.02–61.2	13.2 ± 15.0	0.28	0.31	0.11–10.1	2.57 ± 2.86	0.04	0.06	1.37–60.8	20.1 ± 23.5	0.32	0.36	0.27–2.50	1.10 ± 0.67	0.01	0.02
2-MGA	0.22–2.44	0.91 ± 0.58	0.02	0.02	0.16–2.72	1.02 ± 0.64	0.01	0.02	0.30–3.03	1.31 ± 0.91	0.02	0.02	0.22–2.84	1.22 ± 0.80	0.01	0.02
Subtotal	2.07–76.3	18.3 ± 18.7	0.37	0.42	0.70–15.5	5.07 ± 4.11	0.07	0.10	2.80–88.6	29.5 ± 32.6	0.47	0.52	1.09–7.66	3.56 ± 1.88	0.03	0.05
Monoterpenes-derived SOA tracers																
PNA	0.13–0.78	0.33 ± 0.15	0.01	0.01	0.12–1.87	0.47 ± 0.37	0.01	0.01	0.03–0.64	0.28 ± 0.22	0.01	0.01	0.21–1.59	0.72 ± 0.51	0.01	0.02
PA	0.76–8.32	2.57 ± 1.92	0.07	0.08	0.70–9.06	2.88 ± 1.74	0.05	0.07	0.81–5.90	2.55 ± 1.97	0.06	0.07	0.52–3.91	1.29 ± 1.13	0.02	0.03
3-HGA	0.83–5.26	2.17 ± 1.19	0.04	0.05	0.29–4.29	1.71 ± 1.02	0.02	0.03	1.02–5.95	2.89 ± 2.02	0.05	0.05	0.31–3.44	1.72 ± 1.01	0.01	0.02
3-MBTCA	1.43–8.42	3.45 ± 1.83	0.08	0.09	0.82–8.05	2.88 ± 1.49	0.04	0.06	1.62–11.3	5.28 ± 3.73	0.10	0.11	0.80–8.33	3.18 ± 2.04	0.03	0.06
Subtotal	3.71–19.87	8.52 ± 4.39	0.19	0.22	3.69–16.9	7.94 ± 3.30	0.12	0.17	3.93–22.4	11.0 ± 7.82	0.21	0.24	3.22–13.7	6.91 ± 3.37	0.07	0.13
Sesquiterpenes-derived SOA tracer																
β-Caryophyllinic acid	0.53–2.38	1.26 ± 0.50	0.04	0.04	0.35–5.78	1.72 ± 1.44	0.03	0.04	0.56–2.65	1.44 ± 0.80	0.04	0.05	0.80–4.65	2.53 ± 1.38	0.03	0.05
Total SOA_{Bio} tracers	6.32–98.6	28.0 ± 22.9	0.60	0.69	5.15–31.1	14.7 ± 7.06	0.22	0.31	7.33–113	41.9 ± 40.7	0.72	0.81	5.35–20.5	13.0 ± 5.27	0.13	0.24
Aromatics-derived SOA tracer																
2,3-DHOPA	0.23–1.90	0.86 ± 0.53	0.02	0.02	0.24–6.11	1.75 ± 1.49	0.02	0.02	0.34–3.11	1.42 ± 0.94	0.03	0.03	1.05–2.97	2.02 ± 0.75	0.02	0.03
Total SOA tracers	6.75–100	28.9 ± 23.1	0.62	0.71	5.90–37.2	16.5 ± 8.00	0.23	0.33	8.00–116	43.3 ± 41.5	0.75	0.84	6.40–22.5	15.0 ± 5.51	0.15	0.26
SOC (μg m^{-3})																
SOC_I	0.01–0.10	0.03 ± 0.02	1.43	1.64	0.004–0.03	0.02 ± 0.01	0.48	0.67	0.01–0.18	0.06 ± 0.06	2.21	2.48	0.01–0.03	0.02 ± 0.01	0.31	0.55
SOC_M	0.02–0.09	0.04 ± 0.02	1.67	1.96	0.02–0.07	0.03 ± 0.01	1.00	1.42	0.02–0.10	0.05 ± 0.03	1.87	2.14	0.01–0.06	0.03 ± 0.01	0.64	1.12
SOC_S	0.02–0.10	0.05 ± 0.02	2.48	2.90	0.02–0.25	0.07 ± 0.06	1.73	2.48	0.02–0.12	0.06 ± 0.03	2.61	3.02	0.03–0.20	0.11 ± 0.06	1.98	3.48
SOC_{Bio}	0.05–0.29	0.12 ± 0.06	5.58	6.50	0.04–0.36	0.13 ± 0.08	3.21	4.57	0.05–0.39	0.17 ± 0.12	6.70	7.65	0.06–0.27	0.16 ± 0.07	2.93	5.15
SOC_A	0.03–0.24	0.11 ± 0.07	4.91	5.74	0.03–0.77	0.22 ± 0.19	5.10	7.24	0.04–0.39	0.18 ± 0.12	8.12	9.47	0.13–0.38	0.26 ± 0.10	4.96	8.76
SOC_{Total}	0.10–0.50	0.23 ± 0.12	10.5	12.2	0.07–1.13	0.35 ± 0.26	8.31	11.8	0.13–0.74	0.35 ± 0.24	14.8	17.1	0.20–0.57	0.41 ± 0.15	7.89	13.9

[a]Ave: average; SD: standard deviation; Σ2-MTLs (2-methyltetrols): 2-methylthreitol + 2-methylerythetol; *cis*-2-MTHB: *cis*-2-methyl-1,3,4-trihydroxy-1-butene; 3-MTHB: 3-methyl-2,3,4-trihydroxy-1-butene; *trans*-2-MTHB: *trans*-2-methyl-1,3,4-trihydroxy-1-butene; ΣC_5-alkene triols: *cis*-2-MTHB + 3-MTHB + *trans*-2-MTHB; 2-MGA: 2-methylglyceric acid; PNA: cis-pinonic acid; PA: pinic acid; 3-HGA: 3-hydroxyglutaric acid; 3-MBTCA: 3-methyl-1,2,3-tricarboxylic acid; 2,3-DHOPA: 2,3-dihydroxy-4-oxopentanoic acid; SOC: secondary organic carbon; SOC_I, SOC_M, SOC_S, and SOC_A: SOC derived from isoprene, monoterpenes, sesquiterpenes, and aromatics, respectively.

DOI: 10.1021/acsearthspacechem.9b00170
ACS Earth Space Chem. 2019, 3, 2339−2352

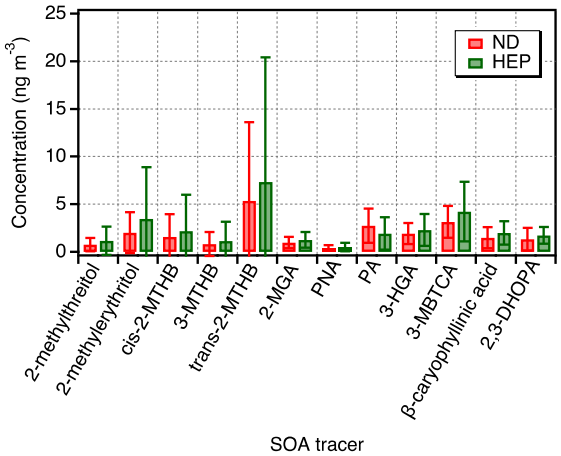

Figure 2. Molecular distributions of biogenic and anthropogenic secondary organic aerosol (SOA) tracers at ND and HEP in Tianjin, North China during the campaign. See Table 1 for abbreviations.

partly derived from biogenic and/or biomass burning sources as well, rather than fossil fuel combustion emissions alone.

Concentrations of total SOA_I tracers and SOA_M observed in Tianjin $PM_{2.5}$ (Table 1) are lower than those (averages 59 ± 32 and 30 ± 14 ng m^{-3}, respectively, at Peking university (PKU) and 75 ± 43 and 32 ± 14 ng m^{-3} at Yufa) reported in the $PM_{2.5}$ collected in summer 2007[52] and 2008[51] (140 ± 101 and 113 ± 63 ng m^{-3} at PKU and 215 ± 160 and 124 ± 48 ng m^{-3} at Yufa) from Beijing. However, concentrations of β-CPA are closer to those (2.7 ± 1.0 ng m^{-3} at PKU and 3.9 ± 1.5 ng m^{-3} at Yufa in summer 2007) reported from Beijing. Similarly, the concentrations of total SOA_I tracers in Tianjin (Table 1) are lower than those (averages 56.5 to 202 ng m^{-3}) reported in summer 2012 from different (urban, suburban, rural, and remote) locations: Hailun, Tongyu, Beijing, Taiyuan, Dunhuang, Shapotou, Hefei, Wuxi, Qianyanzhou, Kunming, Xishuanbanna, Nam Co, and Sanya, but comparable to that (average 26.2 ng m^{-3}) reported from a rural site (Linzhi) over China.[36] In contrast, the concentrations of total SOA_M tracers, β-CPA, and 2,3-DHOPA in Tianjin $PM_{2.5}$ (Table 1) are comparable or even higher than those (averages 0.66 to 9.61 ng m^{-3}, 0.06−3.05 and 0.40−2.40 ng m^{-3}, respectively) reported from 8, 6, and 7 locations, respectively, listed above and slightly lower than those (13.8 to 20.2 ng m^{-3}, 4.98−14.9, and 2.62−5.22 ng m^{-3}, respectively) reported from the rest of the sites located in North, Northeast, and East China in summer 2012.[36]

However, the concentrations of first-generation SOA_I tracers, 2-MTLs, in Tianjin are lower than those reported in forest aerosols collected from Hokkaido, Japan (average 78 ng m^{-3})[66] and Mt. Tai, China (average 98 ng m^{-3})[40] in spring and/or summer periods, where the emission of isoprene from local higher plants is high. However, they are higher than those (1.02 ± 1.17 ng m^{-3}) reported in remote marine aerosols from Okinawa island, Japan, which were considered to be influenced by the aged air masses transported from Asia.[67] Such comparisons suggest that the sources and/or source strength of SOA over Tianjin are significantly distinct from other locations over the northern China plain and that the Tianjin OA might have been influenced by long-range transported aged air masses.

Temporal and Seasonal Variations. Temporal variations in concentrations of SOA tracers determined in $PM_{2.5}$ at ND and HEP in Tianjin during the campaign are depicted in Figure 1e−j. A summary of concentrations of the SOA tracers together with the average contributions of their carbon contents to OC and WSOC in summer and autumn is provided in Table 1. All the SOA tracers including 2,3-DHOPA, except for a few cases, showed very consistent temporal variations with each other at both ND and HEP sites in both seasons and peaked during 14−23 July in summer and were abundant during October, except for 2-MTLs and C_5-alkene triols, in autumn (Figure 1e−j). However, their concentrations, except for a few cases, were slightly higher at HEP than those at ND in summer but comparable, except for PA, in autumn (Figure 1e−j). Interestingly, the concentrations of 2-MTLs and C_5-alkenes were very low from mid-September to October, whereas those of the remaining SOA tracers showed an increasing trend from late September and remained relatively high and stable during October, except for peaks in some cases (Figure 1e−j).

Such spatial and seasonal variations of SOA tracers during the campaign indicate that the origins and formation processes of OA in the Tianjin region are different in summer and autumn. In fact, as noted earlier, the air masses that arrived in Tianjin mostly originated from oceanic regions in the summer, whereas in autumn, they mainly originated from Siberia passing over Mongolia and North China mainland (Figure S2). They should have been enriched with marine biogenic VOCs in the summer and the VOCs emitted from higher plants, biomass burning, and fossil fuel combustion in autumn, and they must have undergone aging during the long-range atmospheric transport. In addition, concentrations of O_3 in the Tianjin atmosphere were higher in summer than in autumn, whereas those of NO_2 were higher in autumn than in summer (Figure 1b), and a similar scenario might have prevailed at the regional scale. Such variations in oxidant loading must have played an important role in formation processes and thus the loading of SOA tracers in each season.

2-MTLs are considered to be specific molecular tracers of isoprene photooxidation in the ambient atmosphere.[68] The 2-MTLS and C_5-alkene triols are mainly formed by reactive uptake of isoprene epoxydiols (IEPOX) that are produced by the reaction of isoprene with OH and HO_2 radicals without the involvement of NO_x.[19,21,69] Besides, 2-MTLs could be produced by isoprene ozonolysis in the presence of acidic aerosol.[70] However, isoprene can be oxidized to methacrolein through RO_2 + NO reaction under high NO_x conditions, which further transforms into methacryloyl peroxynitrate (MPAN) upon oxidation with OH and NO_x radicals.[71,72] MAPN may react with OH to form MGA and related compounds under acidic conditions through the intermediates: MAE[22] and hydroxymethyl-methyl-lactone.[73] The average concentration (8.05 ng m^{-3}) of 2-MTLs at HEP was found to be higher by a factor of ∼2 than that (4.13 ng m^{-3}) at ND in summer. In autumn, their concentrations did not show any significant spatial variations and were lower by 2.7 and 6.5 times than those in summer at ND and HEP, respectively (Table 1). C_5-alkene triols were found to be much higher in summer than that in autumn at both sites, with the highest average concentration of 20.11 ng m^{-3} at HEP in summer (Table 1). Similarly, concentrations of 2-MGA were slightly higher at HEP than those at ND in summer, but such differences were insignificant in autumn (Figure 1f; Table 1). The sum of C_5-alkene triols found to be the most abundant among all isoprene-derived SOA tracers followed by the sum of

DOI: 10.1021/acsearthspacechem.9b00170
ACS Earth Space Chem. 2019, 3, 2339−2352

2-MTLs and 2-MGA, respectively, at both the sites and seasons (Table 1), except in autumn at HEP, in which C_5-alkene triols abundance was found to be the lowest (1.10 ± 0.67 ng m^{-3}).

The high abundances of both 2-MTLs and C_5-alkene triols in summer should have been driven by enhanced emission of isoprene from marine biota and terrestrial vegetation and its subsequent oxidation via HO_2-channel under relatively low NO_x conditions[19−21] (Figure 1b). Whereas in autumn, since the air masses that arrived in Tianjin originated from continental regions (Figure S2), the isoprene contribution from marine biota might be insignificant, despite potential sea-breezes over Tianjin. However, the isoprene emission from higher plants must be reduced with decreasing ambient temperatures (Figure 1a). In addition, the decrease in O_3 and increase in NO_2 concentrations (Figure 1b) must have promoted the formation of 2-MGA via NO_2-channel rather than 2-MTLs and C_5-alkene triols in autumn.[22] Furthermore, the higher levels of all the tracers at HEP than those at ND in summer is likely because the emission of isoprene from local vegetation under high ambient temperatures (Figure 1a) and light must be high in HEP, while no spatial differences in autumn suggests that the influence of local biogenic emission might be insignificant, and thus, the long-range transported air masses might have played a major role.

The scatter plots between 2-methylthreitol and 2-methylerythritol as well as those between 2-MTLs and C_5-alkene triol showed excellent linear relations with high correlation coefficients (r = 0.81 to 0.99) at both ND and HEP in both seasons (see Figure S3a,b). Such linear relations indicate that they should have been derived by similar formation processes in the respective seasons as discussed earlier. The concentration of 2-MGA has been reported to be one order lower than that of 2-MTLs and C_5-alkene triols at low NO_x sites in the US and Germany, as compared to 2−4 times at a rural site, Gucheng, in the North China Plain, where the influence of sulfate, aerosol acidity, and biomass burning was found to be significant.[15] Interestingly, concentrations of 2-MGA were found to be ∼5 times lower than those of 2-MTLs at both sites and more than one order magnitude lower than those of C_5-alkene triols at both sites in summer, whereas in autumn, they were almost similar to those of 2-MTLs at both the sites and those of C_5-alkene triols at HEP (Table 1). Such lower levels of 2-MGA than 2-MTLs and C_5-alkene triols further support that the oxidation of isoprene via HO_2-channel is dominant in summer. In comparison, their similar abundances in autumn implies that the influence of anthropogenic emissions, including biomass burning,[9] should have a severe impact and that the isoprene oxidation via NO_2-channel must be dominant in autumn.

SOA_M tracers (PA, PNA, 3-HGA, and 3-MBTCA) showed very consistent temporal variations in summer at both ND and HEP, and they were similar to those of SOA_I tracers, except for a very few cases (Figure 1e−h), whereas in autumn, the temporal trends of only PA and 3-HGA were found to be similar at both sites, despite the lower levels of PA at HEP and were comparable to that of 2-MGA (Figure 1f−h). Those of PNA and 3-MBTCA were quite different from other SOA_M and SOA_I tracers (Figure 1g,h). Furthermore, the scatter plots of 3-HGA and 3-MBTCA, which are second-generation species of α-pinene, showed a strong linear relationship at both the sites (r = 0.82 at ND and 0.97 at HEP) in only summer, while the correlation coefficients were weak (r = 0.2 and 0.35, respectively) in autumn at both sites (Figure S3c). Concentrations of PNA were higher in autumn than those in summer at both sites (Table 1). In contrast, concentrations of PA in both seasons were comparable at ND, but they were higher in summer than in autumn at HEP (Table 1). Interestingly, both 3-HGA and 3-MBTCA concentrations were higher in summer than in autumn at both sites (Table 1).

Such similarities in temporal trends of both first-generation (PNA and PA) and high-generation (3-HGA and 3-MBTCA) tracers and strong correlations between the 3-HGA and 3-MBTCA indicate that they should have been derived from photooxidation of monoterpenes by O_3 and OH radicals[28,29] under low NO_x conditions in summer. It is likely because the O_3 concentrations were relatively higher and those of NO_2 were lower in summer, as compared to those in autumn in the Tianjin atmosphere (Figure 1b). Moreover, emission of monoterpenes from local vegetation and their subsequent *in situ* photooxidation might be significant, in addition to the contributions from long-range transported air masses that originated from the oceanic regions in summer (Figure S2a,b). In contrast, the differences in temporal trends of the SOA_M tracers and weak correlations between the high-generation tracers in autumn suggest that they must be potentially influenced by additional sources, e.g., biomass burning and anthropogenic pollution, which could influence their formation processes and transformations in the atmosphere. The high abundance of 3-HGA and 3-MBTCA that was formed by photodegradation of PNA and PA[30,31] implies that the aging of OA was higher in summer than in autumn.

β-CPA, the only SOA_S tracer, also showed a very similar temporal trend with all other tracers in summer at both the sites, whereas in autumn, the trend was similar to that of 2-MGA, PA, and 3-HGA as well as 2,3-DHOPA (Figure 1f−j). Further, it was more abundant in autumn than in summer at both sites and the concentration levels were slightly higher at HEP than those at ND (Table 1). It has been reported that because of the low volatility of sesquiterpenes, they could be accumulated in leaves and woods and abundantly emitted by biomass burning.[74] Also, based on the covariance of β-CPA with levoglucosan, it has been considered that the β-CPA loading is increased with increasing biomass burning emissions.[40,75] Hence, the high abundance of β-CPA and its covariance with levoglucosan in Tianjin $PM_{2.5}$ in autumn suggests that VOCs emitted from biomass burning should have played a prominent role in enhancing its loading in the Tianjin atmosphere rather than through biogenic emissions. The extremely low levels of 2-MTLs and C_5-alkene triols in autumn also indicates that the contribution of SOA from biogenic emissions was low in autumn. Details of the possible influence of biomass burning is described in the next section.

2,3-DHOPA, the only SOA_A tracer, showed very similar temporal variations, including peaks during July and October, with those of all the biogenic SOA tracers in summer at both the sites (Figure 1e-j). Such covariance might have been driven by high oxidation capacity of the atmosphere over Tianjin that results in the enhanced formation of SOA originating from both biogenic and anthropogenic origins. However, the concentrations of oxidants (e.g., O_3 and NO_2) in Tianjin were not enhanced during July 14−23, nor in October, corresponding to the peaks in SOA tracers, which suggests that the temporal trends of Tianjin OA might have mainly been influenced by long-range transported air masses rather than local emissions. Interestingly, the air masses that arrived in

DOI: 10.1021/acsearthspacechem.9b00170
ACS Earth Space Chem. 2019, 3, 2339−2352

Tianjin in July mostly originated from the oceanic regions (Figure S2a) that should have been enriched with marine biogenic emissions. Furthermore, the concentrations of 2,3-DHOPA were found to be higher at HEP, where the emission of biogenic VOCs should be higher, than those at ND, where fossil fuel combustion should be relatively higher (Table 1; Figure 1j). Surprisingly, in autumn, the temporal trend of 2,3-DHOPA was found to be extremely similar to that of β-CPA, 3-HGA, and 2-MGA at ND and also at HEP, except for a few cases (Figure 1f,h−j). These results suggest that DHOPA might be partly derived from biogenic and biomass burning emissions, rather than fossil fuel combustion alone. Such a possibility is discussed in the following sections.

Mass ratios of first-generation to high-generation products such as Σ(2-MTLS + C_5-alkene triols)/2-MGA and Σ(PNA + PA)/Σ(3-HGA + 3-MBTCA) were 17.8 ± 9.07 and 0.53 ± 0.36 at ND and 18.1 ± 10.8 and 0.35 ± 0.08 at HEP, respectively, in summer and 4.38 ± 3.63 and 0.81 ± 0.42 at ND and 2.25 ± 0.82 and 0.56 ± 0.53 at HEP in autumn. Scatter plots between these mass ratios and ambient temperatures and RH at Tianjin were very scattered and did not show a linear relationship, except between the Σ(2-MTLS + C_5-alkene triols)/2-MGA and temperature in summer at both the sites and at ND in autumn, as opposed to an inverse relation at HEP (Figure S4). Such high mass ratios of Σ(2-MTLS + C_5-alkene triols)/2-MGA and linear relations with temperature indicate that the emission of BVOCs and subsequent *in situ* photochemical formation of SOA, particularly SOA_I, at the local scale should be significant over Tianjin in summer. However, the lower Σ(PNA + PA)/Σ(3-HGA + 3-MBTCA) ratios and their lack of relation with local meteorological parameters further suggest that the SOA loading over Tianjin was not only influenced by local biogenic emissions but also by the long-range transported air masses in both seasons.

Enhanced Contribution of Biogenic VOCs in Summer. Temporal variations of SOA tracers, except for MTLs and C_5-alkene triols in autumn (Figure 1e−j), were consistent with not only those of WSOC and OC but also EC (Figure 1c). Such comparability implies that the loading of SOA in Tianjin is mainly controlled by VOC emission strength rather than the local meteorology. However, the concentrations of all the SOA tracers, as well as WSOC, OC, and even EC, were enhanced in the samples collected during 14−23 July at both sites in summer, although the increase in the EC level was not as high as WSOC or OC (Figure 1c,e−j). Concentrations of a sum of hopanoid hydrocarbons (C_{27-32}), molecular markers for fossil fuel combustion emissions,[76,77] were found to be very low and did not show any increase during these days, but for levoglucosan, an excellent tracer for biomass burning,[64] levels were slightly enhanced during these days (Figure 1d). Hence, biomass burning emissions might have caused the enhancement of EC levels, as well as organics, in summer. However, the loading of levoglucosan was much lower in summer (range, 0.77−26.9 ng m^{-3} at ND and 0.31−8.96 ng m^{-3} at HEP) than in autumn (6.94−210 and 28.4−203 ng m^{-3}, respectively), which implies that the emissions from biomass burning should be minor in summer. Hence, it is likely that the loading of organics over Tianjin in summer should have been mainly driven by biogenic emission of VOCs and their subsequent photooxidation.

It has been well identified that increasing ambient temperature and solar intensity increases the stress on higher plants and biological activity over the sea surface and that it therefore enhances the emission of VOCs from terrestrial vegetation and marine biota in summer.[11] Furthermore, increased ambient temperature and RH promotes the photochemical oxidation of VOCs and phase transition, respectively, to produce SOA. The ambient temperature in Tianjin was relatively increased, and RH was lower than 80% during 14−23 July (Figure 1a), corresponding to the peaks in SOA tracers as well as OC and WSOC (Figures.1c,e−j). It is likely that the same scenario might have prevailed at regional scale. Scatter plots of total isoprene- and α/β-pinene-derived SOA tracers with ambient temperature showed a linear relationship with weak to moderate correlation coefficients in both summer and autumn (Figure S5). Whereas β-caryophyllinic acid and 2,3-DHOPA, except at ND, showed a linear relationship with temperature in summer and an inverse relationship in autumn (Figure S5i,k,m,o). Interestingly, all the SOA tracers showed a linear relationship with RH in autumn with weak to moderate correlation coefficients, in which the RH did not exceed 75%, (Figure S 5d,h,l,p), but not in summer (Figure S5b,f,j,n). It is worthy to note that the data points showed a positive trend until the RH reaches 70% in summer, after that they were scattered (Figure S5b,f,j,n).

Such trends and linear relationships imply that the enhanced emission and photochemical oxidation of BVOCs are a significant source of SOA over Tianjin in summer, whereas in autumn, the SOA should be derived from other sources as well. However, the gas-to-particle partitioning might be significant in autumn. In summer, the gas-to-particle partitioning might be enhanced with increasing RH up to only ∼75%, and after that, the aqueous phase reactions may become more prominent resulting in the high-generation more oxygenated products.

Influence of Biomass Burning and Fossil Fuel Combustion. To understand the role of biomass burning and fossil fuel combustion emissions on SOA loading and its formation processes over Tianjin, we examined linear relationships between SOA tracers and specific tracers: levoglucosan and hopanes, for the biomass burning[64] and fossil fuel combustion,[76,77] respectively. We found that the scatter plots of both isoprene- and α/β-pinene-derived SOA tracers with levoglucosan were highly scattered and did not show any relation at either site in summer and autumn (Figure S6). Although temporal variations of β-CPA (Figure 1i) are not similar to those of levoglucosan, which were found to be significant only from early September and abundant during October (Figure 1d), they showed linear relations with weak or moderate correlation coefficients at both sites and in both seasons (Figure 3). Such linear relationships suggest that β-CPA should have been partly derived from the VOCs emitted from biomass burning, particularly in autumn. However, the air masses that arrived in Tianjin originated from Siberia and passed over Mongolia and the mainland of northern China where possible biomass emissions, including crop waste burning, are high in autumn. Moreover, concentrations of NO_2 increased in autumn compared to those in summer, and the temporal pattern (Figure 1b) was very close to that of both levoglucosan and β-CPA (Figure 1d,i), which further supports our assumption that biomass burning emissions were significant in autumn.

2,3-DHOPA showed positive relationships with hopanes at both sites in both seasons, but the correlation coefficients were weak or moderate (Figure 4a,b). Interestingly, it also showed

DOI: 10.1021/acsearthspacechem.9b00170
ACS Earth Space Chem. 2019, 3, 2339−2352

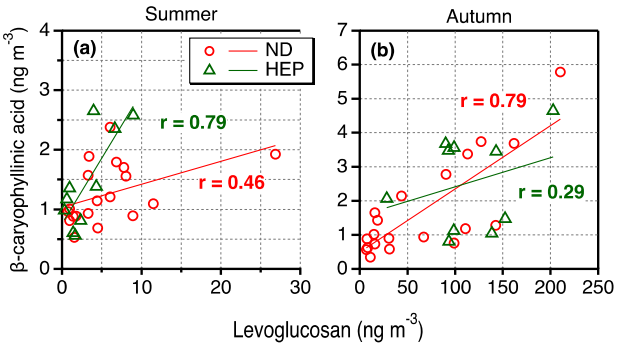

Figure 3. Scatter plots between β-caryophyllinic acid and levoglucosan, a marker for biomass burning, at ND and HEP in Tianjin in summer (a) and autumn (b).

linear relationships with levoglucosan with moderate to good correlation coefficients in both seasons at ND and in summer at HEP (Figure 4c,d). However, 2,3-DHOPA showed linear relationships with β-CPA with high correlation coefficients in both summer and autumn (Figure 4e,f). These results, together with the covariance with biogenic SOA tracers, particularly in summer (Figure 1e–j), suggest that 2,3-DHOPA in Tianjin $PM_{2.5}$ should have been derived not only from fossil fuel combustion but also partly from biogenic emissions and biomass burning. It is likely because terrestrial higher plants,[78] marine biota,[79] and wood combustion[80] emit significant amounts of phenolic compounds that could produce the 2,3-DHOPA upon photooxidation in the atmosphere. However, such a possibility needs to be investigated further, a subject of future research.

Contributions of SOA Tracers to OC and WSOC. Contributions of total isoprene-derived SOA tracers-C contents to OC and WSOC were found to be more abundant in summer at both ND (range, 0.07–1.16% and 0.07–1.21%, respectively) and HEP (0.14–1.20% and 0.17–1.15%) followed by those of α/β-pinene-derived SOA tracers (0.09–0.37% and 0.12–0.48% at ND and 0.09–0.29% and 0.11–0.29% at HEP, respectively), β-caryophyllinic acid and 2,3-DHOPA, respectively (Table 1), whereas in autumn, the contributions of α/β-pinene-derived SOA tracers-C in OC (0.06–0.21% at ND and 0.04–0.19% at HEP) and WSOC (0.09–0.32% and 0.06–0.37%, respectively) were abundant followed by those of isoprene-derived SOA tracers (0.01–0.23% and 0.02–0.29% at ND and 0.01–0.07% and 0.03–0.13% at HEP, respectively), β-CPA and 2,3-DHOPA, respectively (Table 1). These trends indicate that isoprene-derived SOA tracers largely contribute to organics in summer, as opposed to monoterpene-derived SOA tracers in autumn over Tianjin.

Source Apportionment by SOA-Tracer Method. The SOA-tracer based method developed by Kleindienst et al.[35] was applied to estimate the contributions of SOC derived from isoprene (SOC_I), monoterpene (SOC_M), sesquiterpene (SOC_S), and aromatics (SOC_A) using the measured concentrations of SOA tracers. A summary of the estimated SOC_I, SOC_M, SOC_S, and SOC_A and their average contributions to OC and WSOC at ND and HEP in summer and autumn is provided in Table 1. Their temporal variations are depicted in Figure 5. The SOC_I ranged from 0.004 to 0.097 μgC m^{-3} with an average of 0.024 ± 0.020 μgC m^{-3} at ND and 0.005–0.183 μgC m^{-3} (average 0.038 ± 0.048 μgC m^{-3}) at HEP, while the SOC_M and SOC_S were 0.016–0.086 μgC m^{-3} (0.036 ± 0.017 μgC m^{-3}) and 0.015–0.251 μgC m^{-3} (0.065 ± 0.048 μg m^{-3}) at ND and 0.014–0.097 μgC m^{-3} (0.039 ± 0.027 μg m^{-3}) and 0.024–0.202 μgC m^{-3} (0.086 ± 0.054 μgC m^{-3}) at HEP, respectively. The SOC_A was 0.029–0.774 μgC m^{-3} (0.167 ± 0.152 μgC m^{-3}) at ND and 0.043–0.394 μgC m^{-3} (0.218 ± 0.112 μgC m^{-3}) at HEP. SOC_A was found to be the most abundant component that accounted for 45 ± 11% of total SOC at ND and 51 ± 12% at HEP in summer and 60 ± 10% and 63 ± 7%, respectively, in autumn followed by SOC_S

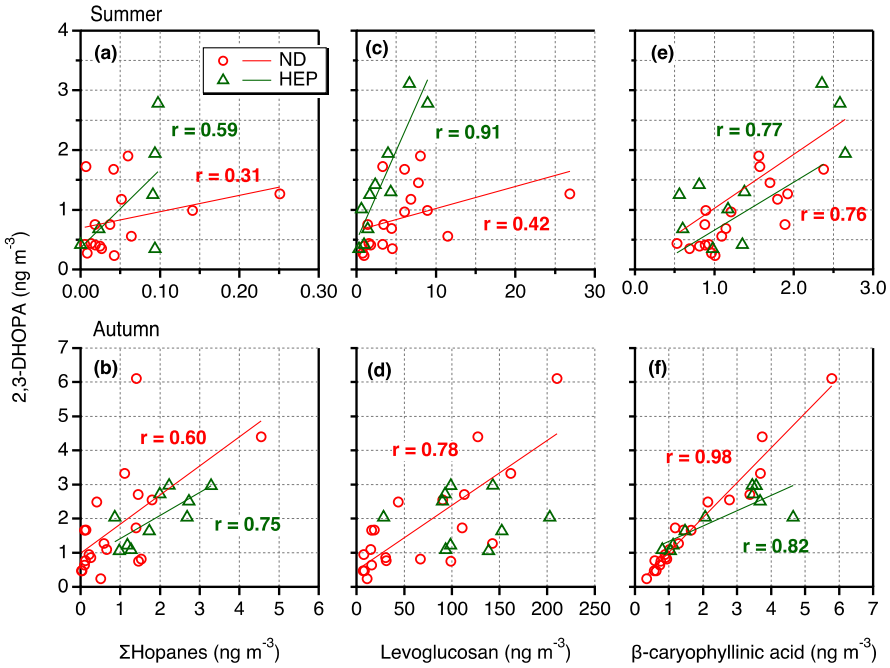

Figure 4. Scatter plots of DHOPA with hopanes (a,b), levoglucosan (c,d), and β-caryophyllinic acid (e,f) at ND and HEP in Tianjin in summer and autumn.

DOI: 10.1021/acsearthspacechem.9b00170
ACS Earth Space Chem. 2019, 3, 2339–2352

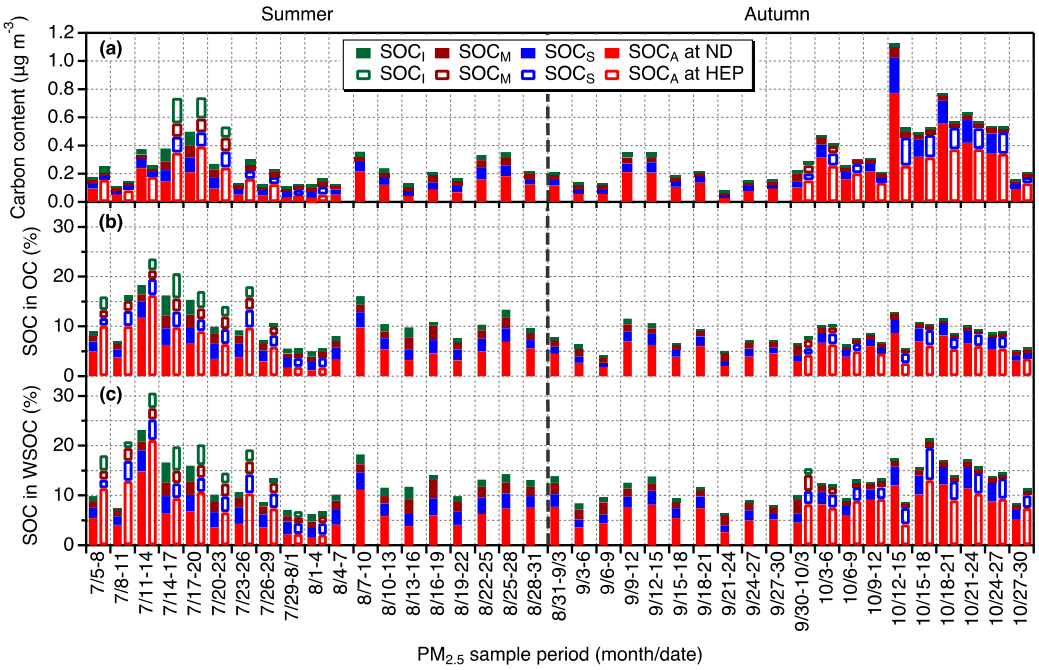

Figure 5. Temporal variations in concentrations (μg m^{-3}) of SOC derived from isoprene (SOCI), monoterpene (SOCM), sesquiterpene (SOCS), and aromatics (SOCA) (a) and their contributions to OC (b) and WSOC (c) in $PM_{2.5}$ at ND and HEP in Tianjin during summer to autumn.

(25 ± 6% and 20 ± 8% in summer and 21 ± 3% and 25 ± 6% in autumn) at both sites during the campaign. SOA_M was the third most abundant (17 ± 5%) at ND in summer and at both the sites (13 ± 8% and 8 ± 5%, respectively) in autumn, whereas SOA_I was the third most abundant at HEP (15 ± 6%) in summer. These results indicate that the total biogenic SOC accounts for ∼50% in summer and ∼40% in autumn, while the rest would be derived from aromatics of anthropogenic sources including biomass burning. However, the possible biogenic origin of 2,3-DHOPA and thus SOC_A needs to be investigated further.

The SOC_I and SOC_M loadings were higher at HEP than that at ND in summer, whereas in autumn, they did not show any significant spatial variation but were much lower as compared to summer (Table 1). In contrast, both SOC_S and SOC_A were higher in autumn than in summer at both sites and were also higher at HEP than at ND in both seasons (Table 1). Although the temporal variations in SOC were peaked in mid-July in summer and during October in autumn, their contributions to OC and WSOC were relatively stable: accounting for ∼10% and ∼15%, respectively, during the whole campaign period except for a few cases (Figure 5). This suggests that SOA formation is always significant and plays a major role in driving the OA burden in the Tianjin region. The contribution of total SOC (SOC_{Total}) ranged from 5.06% to 18.4% with an average of 10.5 ± 3.76% to OC at ND, 5.59−23.7% (average 14.8 ± 5.97%) at HEP in summer and 4.16−12.7 (8.31 ± 2.45%) and 5.21−10.3% (7.89 ± 1.77%), respectively, in autumn, while the contributions of SOC_{Total} to WSOC were 6.28−23.2% (12.2 ± 4.21%) at ND and 6.84−30.7% (17.1 ± 7.09%) at HEP in summer and 6.46−17.5% (11.8 ± 3.32%) and 8.64−21.3% (13.9 ± 3.32%), respectively, in autumn. Thus, it is clear that the contributions of SOC to both WSOC and OC are significant over the Tianjin region and enhanced in summer due to increased emissions of biogenic VOCs and photochemical activity due to high ambient temperatures and solar intensity in summer.

■ CONCLUSIONS

The consistent temporal variations, except for a few cases, of all the measured SOA tracers including 2,3-DHOPA at both sites with peaks during 14−23 July, corresponding to high ambient temperatures in Tianjin, and their relatively high abundance at a background site (HEP) as compared to an urban site (ND) implied that biogenic emissions from local vegetation and subsequent SOA formation were high in summer, while the high loadings of all the tracers, except for 2-MTLs and C_5-alkene triols, during October, corresponding to levoglucosan, a marker of biomass burning, indicate that the contributions of the SOA derived from the biomass burning emissions were significant in autumn. The relationships between 2,3-DHOPA and hopanes and no relation of the mass ratios of first- to high-generation SOA tracers and meteorological parameters suggested that the contributions from anthropogenic aromatics and aging of OA during long-range transport over the Tianjin region were significant in both seasons. The estimated contributions of SOC indicated that the SOC derived from anthropogenic aromatics was abundant (∼50% in summer and ∼60% in autumn) over Tianjin, North China. Based on the covariance of 2,3-DHOPA with biogenic SOA tracers, and the linear relation with β-CPA together with its high abundance at HEP and origins of the air masses arrived in Tianjin, we conclude that the 2,3-DHOPA was partly derived from biogenic and biomass burning emissions. However, it needs to be confirmed through further investigation, a subject of future research.

■ ASSOCIATED CONTENT

Ⓢ Supporting Information

The Supporting Information is available free of charge on the ACS Publications website at DOI: 10.1021/acsearthspacechem.9b00170.

Map of China with sampling sites, air mass trajectories, and scatter plots of selected SOA tracers versus the

DOI: 10.1021/acsearthspacechem.9b00170
ACS Earth Space Chem. 2019, 3, 2339−2352

tracers and levoglucosan, and those of tracers as well as their mass ratios and ambient temperature and RH (Figures S1−S6) (PDF)

■ AUTHOR INFORMATION

Corresponding Author

*Phone: +86 22 87370995. E-mail: cmpavuluri@tju.edu.cn.

ORCID

Chandra Mouli Pavuluri: 0000-0002-2955-474X
Pingqing Fu: 0000-0001-6249-2280
Yan-Lin Zhang: 0000-0002-8722-8635

Notes

The authors declare no competing financial interest.

■ ACKNOWLEDGMENTS

This study was in part supported by The National Natural Science Foundation of China through Grant-in-Aid numbers: 41775120 and 91644103, and the National Key R&D Program of China (2017YFC0212700).

■ REFERENCES

(1) Kanakidou, M.; Seinfeld, J. H.; Pandis, S. N.; Barnes, I.; Dentener, F. J.; Facchini, M. C.; Van Dingenen, R.; Ervens, B.; Nenes, A.; Nielsen, C. J.; Swietlicki, E.; Putaud, J. P.; Balkanski, Y.; Fuzzi, S.; Horth, J.; Moortgat, G. K.; Winterhalter, R.; Myhre, C. E. L.; Tsigaridis, K.; Vignati, E.; Stephanou, E. G.; Wilson, J. Organic aerosol and global climate modelling: a review. *Atmos. Chem. Phys.* **2005**, *5*, 1053−1123.

(2) Ramanathan, V.; Crutzen, P. J.; Kiehl, J. T.; Rosenfeld, D. Aerosols, Climate, and the Hydrological Cycle. *Science* **2001**, *294*, 2119−2124.

(3) Baltensperger, U.; Dommen, J.; Alfarra, R.; Duplissy, J.; Gaeggeler, K.; Metzger, A.; Facchini, M. C.; Decesari, S.; Finessi, E.; Reinnig, C.; Schott, M.; Warnke, J.; Hoffmann, T.; Klatzer, B.; Puxbaum, H.; Geiser, M.; Savi, M.; Lang, D.; Kalberer, M.; Geiser, T. Combined determination of the chemical composition and of health effects of secondary organic aerosols: The POLYSOA project. *J. Aerosol Med. Pulm. Drug Delivery* **2008**, *21* (1), 145−154.

(4) Tuet, W. Y.; Chen, Y. L.; Fok, S.; Champion, J. A.; Ng, N. L. Inflammatory responses to secondary organic aerosols (SOA) generated from biogenic and anthropogenic precursors. *Atmos. Chem. Phys.* **2017**, *17* (18), 11423−11440.

(5) Andreae, M. O.; Crutzen, P. J. Atmospheric aerosols: Biogeochemical sources and role in atmospheric chemistry. *Science* **1997**, *276* (5315), 1052−1058.

(6) Fu, T. M.; Jacob, D. J.; Wittrock, F.; Burrows, J. P.; Vrekoussis, M.; Henze, D. K. Global budgets of atmospheric glyoxal and methylglyoxal, and implications for formation of secondary organic aerosols. *J. Geophys. Res.* **2008**, *113* (D15), D15303.

(7) Robinson, A. L.; Donahue, N. M.; Shrivastava, M. K.; Weitkamp, E. A.; Sage, A. M.; Grieshop, A. P.; Lane, T. E.; Pierce, J. R.; Pandis, S. N. Rethinking organic aerosols: Semivolatile emissions and photochemical aging. *Science* **2007**, *315* (5816), 1259−1262.

(8) Hallquist, M.; Wenger, J. C.; Baltensperger, U.; Rudich, Y. The formation, properties and impact of secondary organic aerosol: current and emerging issues. *Atmos. Chem. Phys.* **2009**, *9*, 5155−5236.

(9) Ding, X.; He, Q. F.; Shen, R. Q.; Yu, Q. Q.; Zhang, Y. Q.; Xin, J. Y.; Wen, T. X.; Wang, X. M. Spatial and seasonal variations of isoprene secondary organic aerosol in China: Significant impact of biomass burning during winter. *Sci. Rep.* **2016**, *6*, 20411.

(10) Ding, X.; Zhang, Y. Q.; He, Q. F.; Yu, Q. Q.; Shen, R. Q.; Zhang, Y. L.; Zhang, Z.; Lyu, S. J.; Hu, Q. H.; Wang, Y. S.; Li, L. F.; Song, W.; Wang, X. M. Spatial and seasonal variations of secondary organic aerosol from terpenoids over China. *J. Geophys Res-Atmos* **2016**, *121* (24), 14661−14678.

(11) Guenther, A.; Hewitt, C. N.; Erickson, D.; Fall, R.; Geron, C.; Graedel, T.; Harley, P.; Lklinger, L.; Lerdau, M.; McKay, W. A.; Pierce, T.; Scholes, B.; Steinbrecher, R.; Tallamraju, R.; Taylor, J.; Zimmerman, P. A global model of natural volatile organic compound emissions. *J. Geophys. Res.* **1995**, *100*, 8873−8892.

(12) Guenther, A.; Karl, T.; Harley, P.; Wiedinmyer, C.; Palmer, P. I.; Geron, C. Estimates of global terrestrial isoprene emissions using MEGAN (Model of Emissions of Gases and Aerosols from Nature). *Atmos. Chem. Phys.* **2006**, *6*, 3181−3210.

(13) Piccot, S.; Watson, J. G.; Jones, J. A global inventory of volatile organic compound emissions from anthropogenic sources. *Journal of Geophysical Research* **1992**, *97* (D9), 9897−9912.

(14) de Gouw, J.; Jimenez, J. L. Organic Aerosols in the Earth's Atmosphere. *Environ. Sci. Technol.* **2009**, *43* (20), 7614−7618.

(15) Li, J. J.; Wang, G. H.; Wu, C.; Cao, C.; Ren, Y. Q.; Wang, J. Y.; Li, J.; Cao, J. J.; Zeng, L. M.; Zhu, T. Characterization of isoprene-derived secondary organic aerosols at a rural site in North China Plain with implications for anthropogenic pollution effects. *Sci. Rep.* **2018**, *8*, 535.

(16) Hoyle, C. R.; Boy, M.; Donahue, N. M.; Fry, J. L.; Glasius, M.; Guenther, A.; Hallar, A. G.; Hartz, K. H.; Petters, M. D.; Petaja, T.; Rosenoern, T.; Sullivan, A. P. A review of the anthropogenic influence on biogenic secondary organic aerosol. *Atmos. Chem. Phys.* **2011**, *11* (1), 321−343.

(17) Pandis, S. N.; Paulson, S. E.; Seinfeld, J. H.; Flagan, R. C. Aerosol formation in the photooxidation of isoprene and β-pinene. *Atmos. Environ., Part A* **1991**, *25A*, 997−1008.

(18) Claeys, M.; Graham, B.; Vas, G.; Wang, W.; Vermeylen, R.; Pashynska, V.; Cafmeyer, J.; Guyon, P.; Andreae, M. O.; Artaxo, P.; Maenhaut, W. Formation of secondary organic aerosols through photooxidation of isoprene. *Science* **2004**, *303* (5661), 1173−1176.

(19) Paulot, F.; Crounse, J. D.; Kjaergaard, H. G.; Kurten, A.; St Clair, J. M.; Seinfeld, J. H.; Wennberg, P. O. Unexpected Epoxide Formation in the Gas-Phase Photooxidation of Isoprene. *Science* **2009**, *325* (5941), 730−733.

(20) Lin, Y. H.; Zhang, Z.; Docherty, K. S.; Zhang, H.; Budisulistiorini, S. H.; Rubitschun, C. L.; Shaw, S. L.; Knipping, E. M.; Edgerton, E. S.; Kleindienst, T. E.; Gold, A.; Surratt, J. D. Isoprene epoxydiols as precursors to secondary organic aerosol formation: acid-catalyzed reactive uptake studies with authentic compounds. *Environ. Sci. Technol.* **2012**, *46* (1), 250−8.

(21) Surratt, J. D.; Chan, A. W. H.; Eddingsaas, N. C.; Chan, M. N.; Loza, C. L.; Kwan, A. J.; Hersey, S. P.; Flagan, R. C.; Wennberg, P. O.; Seinfeld, J. H. Reactive intermediates revealed in secondary organic aerosol formation from isoprene. *Proc. Natl. Acad. Sci. U. S. A.* **2010**, *107* (15), 6640−6645.

(22) Lin, Y. H.; Zhang, H. F.; Pye, H. O. T.; Zhang, Z. F.; Marth, W. J.; Park, S.; Arashiro, M.; Cui, T. Q.; Budisulistiorini, H.; Sexton, K. G.; Vizuete, W.; Xie, Y.; Luecken, D. J.; Piletic, I. R.; Edney, E. O.; Bartolotti, L. J.; Gold, A.; Surratt, J. D. Epoxide as a precursor to secondary organic aerosol formation from isoprene photooxidation in the presence of nitrogen oxides. *Proc. Natl. Acad. Sci. U. S. A.* **2013**, *110* (17), 6718−6723.

(23) Zhang, H.; Surratt, J. D.; Lin, Y. H.; Bapat, J.; Kamens, R. M. Effect of relative humidity on SOA formation from isoprene/NO photooxidation: enhancement of 2-methylglyceric acid and its corresponding oligoesters under dry conditions. *Atmos. Chem. Phys.* **2011**, *11* (13), 6411−6424.

(24) Surratt, J. D.; Lewandowski, M.; Offenberg, J. H.; Jaoui, M.; Kleindienst, T. E.; Edney, E. O.; Seinfeld, J. H. Effect of acidity on secondary organic aerosol formation from isoprene. *Environ. Sci. Technol.* **2007**, *41* (15), 5363−5369.

(25) Carlton, A. G.; Wiedinmyer, C.; Kroll, J. H. A review of Secondary Organic Aerosol (SOA) formation from isoprene. *Atmos. Chem. Phys.* **2009**, *9* (14), 4987−5005.

(26) Heald, C. L.; Henze, D. K.; Horowitz, L. W.; Feddema, J.; Lamarque, J. F.; Guenther, A.; Hess, P. G.; Vitt, F.; Seinfeld, J. H.; Goldstein, A. H.; Fung, I. Predicted change in global secondary organic aerosol concentrations in response to future climate,

DOI: 10.1021/acsearthspacechem.9b00170
ACS Earth Space Chem. 2019, 3, 2339−2352

emissions, and land use change. *J. Geophys Res-Atmos* **2008**, *113* (D5), D05211.
(27) Kanakidou, M.; Seinfeld, J. H.; Pandis, S. N. Organic aerosol and global climate modelling, a review.pdf. *Atmos. Chem. Phys.* **2005**, *5*, 1053−1123.
(28) Jenkin, M. E.; Shallcross, D. E.; Harvey, J. N. Development and application of a possible mechanism for the generation of cis-pinic acid from the ozonolysis of alpha- and beta-pinene. *Atmos. Environ.* **2000**, *34* (18), 2837−2850.
(29) Larsen, B. R.; Di Bella, D.; Glasius, M.; Winterhalter, R.; Jensen, N. R.; Hjorth, J. Gas-phase OH oxidation of monoterpenes: Gaseous and particulate products. *J. Atmos. Chem.* **2001**, *38* (3), 231−276.
(30) Muller, L.; Reinnig, M. C.; Naumann, K. H.; Saathoff, H.; Mentel, T. F.; Donahue, N. M.; Hoffmann, T. Formation of 3-methyl-1,2,3-butanetricarboxylic acid via gas phase oxidation of pinonic acid - a mass spectrometric study of SOA aging. *Atmos. Chem. Phys.* **2012**, *12* (3), 1483−1496.
(31) Claeys, M.; Szmigielski, R.; Kourtchev, I.; Van der Veken, P.; Vermeylen, R.; Maenhaut, W.; Jaoui, M.; Kleindienst, T. E.; Lewandowski, M.; Offenberg, J. H.; Edney, E. O. Hydroxydicarboxylic acids: Markers for secondary organic aerosol from the photooxidation of alpha-pinene. *Environ. Sci. Technol.* **2007**, *41* (5), 1628−1634.
(32) Jaoui, M.; Lewandowski, M.; Kleindienst, T. E.; Offenberg, J. H.; Edney, E. O. beta-caryophyllinic acid: An atmospheric tracer for beta-caryophyllene secondary organic aerosol. *Geophys. Res. Lett.* **2007**, *34* (5), L05816.
(33) Hallquist, M.; Wenger, J. C.; Baltensperger, U.; Rudich, Y.; Simpson, D.; Claeys, M.; Dommen, J.; Donahue, N. M.; George, C.; Goldstein, A. H.; Hamilton, J. F.; Herrmann, H.; Hoffmann, T.; Iinuma, Y.; Jang, M.; Jenkin, M. E.; Jimenez, J. L.; Kiendler-Scharr, A.; Maenhaut, W.; McFiggans, G.; Mentel, T. F.; Monod, A.; Prevot, A. S. H.; Seinfeld, J. H.; Surratt, J. D.; Szmigielski, R.; Wildt, J. The formation, properties and impact of secondary organic aerosol: current and emerging issues. *Atmos. Chem. Phys.* **2009**, *9* (14), 5155−5236.
(34) Offenberg, J. H.; Lewis, C. W.; Lewandowski, M.; Jaoui, M.; Kleindienst, T. E.; Edney, E. O. Contributions of toluene and alpha-pinene to SOA formed in an irradiated toluene/alpha-pinene/NOx/air mixture: Comparison of results using C-14 content and SOA organic tracer methods. *Environ. Sci. Technol.* **2007**, *41* (11), 3972−3976.
(35) Kleindienst, T. E.; Jaoui, M.; Lewandowski, M.; Offenberg, J. H.; Lewis, C. W.; Bhave, P. V.; Edney, E. O. Estimates of the contributions of biogenic and anthropogenic hydrocarbons to secondary organic aerosol at a southeastern US location. *Atmos. Environ.* **2007**, *41* (37), 8288−8300.
(36) Ding, X.; He, Q. F.; Shen, R. Q.; Yu, Q. Q.; Wang, X. M. Spatial distributions of secondary organic aerosols from isoprene, monoterpenes, beta-caryophyllene, and aromatics over China during summer. *J. Geophys Res-Atmos* **2014**, *119* (20), 11877−11891.
(37) Kavouras, I. G.; Mihalopoulos, N.; Stephanou, E. G. Formation of atmospheric particles from organic acids produced by forests. *Nature* **1998**, *395* (6703), 683−686.
(38) Cahill, T. M.; Seaman, V. Y.; Charles, M. J.; Holzinger, R.; Goldstein, A. H. Secondary organic aerosols formed from oxidation of biogenic volatile organic compounds in the Sierra Nevada Mountains of California. *J. Geophys. Res.* **2006**, *111* (D16), D16312.
(39) Wang, W.; Wu, M. H.; Li, L.; Zhang, T.; Liu, X. D.; Feng, J. L.; Li, H. J.; Wang, Y. J.; Sheng, G. Y.; Claeys, M.; Fu, J. M. Polar organic tracers in PM2.5 aerosols from forests in eastern China. *Atmos. Chem. Phys.* **2008**, *8* (24), 7507−7518.
(40) Fu, P.; Kawamura, K.; Kanaya, Y.; Wang, Z. Contributions of biogenic volatile organic compounds to the formation of secondary organic aerosols over Mt. Tai, Central East China. *Atmos. Environ.* **2010**, *44* (38), 4817−4826.
(41) Fu, P. Q.; Kawamura, K. Diurnal variations of polar organic tracers in summer forest aerosols: A case study of a Quercus and Picea mixed forest in Hokkaido, Japan. *Geochem. J.* **2011**, *45* (4), 297−308.
(42) Shen, R. Q.; Ding, X.; He, Q. F.; Cong, Z. Y.; Yu, Q. Q.; Wang, X. M. Seasonal variation of secondary organic aerosol tracers in Central Tibetan Plateau. *Atmos. Chem. Phys.* **2015**, *15* (15), 8781−8793.
(43) Hu, D.; Bian, Q.; Li, T. W. Y.; Lau, A. K. H.; Yu, J. Z. Contributions of isoprene, monoterpenes, beta-caryophyllene, and toluene to secondary organic aerosols in Hong Kong during the summer of 2006. *J. Geophys. Res.* **2008**, *113*, D22206.
(44) Ding, X.; Zheng, M.; Yu, L. P.; Zhang, X. L.; Weber, R. J.; Yan, B.; Russell, A. G.; Edgerton, E. S.; Wang, X. M. Spatial and seasonal trends in biogenic secondary organic aerosol tracers and water-soluble organic carbon in the southeastern United States. *Environ. Sci. Technol.* **2008**, *42* (14), 5171−5176.
(45) Fu, P. Q.; Kawamura, K.; Pavuluri, C. M.; Swaminathan, T.; Chen, J. Molecular characterization of urban organic aerosol in tropical India: contributions of primary emissions and secondary photooxidation. *Atmos. Chem. Phys.* **2010**, *10*, 2663−2689.
(46) Fu, P. Q.; Kawamura, K.; Chen, J.; Barrie, L. A. Isoprene, Monoterpene, and Sesquiterpene Oxidation Products in the High Arctic Aerosols during Late Winter to Early Summer. *Environ. Sci. Technol.* **2009**, *43* (11), 4022−4028.
(47) Chai, F. H.; Gao, J.; Chen, Z. X.; Wang, S. L.; Zhang, Y. C.; Zhang, J. Q.; Zhang, H. F.; Yun, Y. R.; Ren, C. Spatial and temporal variation of particulate matter and gaseous pollutants in 26 cities in China. *J. Environ. Sci.* **2014**, *26* (1), 75−82.
(48) Huang, R. J.; Zhang, Y. L.; Bozzetti, C.; Ho, K. F.; Cao, J. J.; Han, Y. M.; Daellenbach, K. R.; Slowik, J. G.; Platt, S. M.; Canonaco, F.; Zotter, P.; Wolf, R.; Pieber, S. M.; Bruns, E. A.; Crippa, M.; Ciarelli, G.; Piazzalunga, A.; Schwikowski, M.; Abbaszade, G.; Schnelle-Kreis, J.; Zimmermann, R.; An, Z. S.; Szidat, S.; Baltensperger, U.; El Haddad, I.; Prevot, A. S. H. High secondary aerosol contribution to particulate pollution during haze events in China. *Nature* **2014**, *514* (7521), 218−222.
(49) Jiang, F.; Liu, Q.; Huang, X. X.; Wang, T. J.; Zhuang, B. L.; Xie, M. Regional modeling of secondary organic aerosol over China using WRF/Chem. *J. Aerosol Sci.* **2012**, *43* (1), 57−73.
(50) Fu, T. M.; Cao, J. J.; Zhang, X. Y.; Lee, S. C.; Zhang, Q.; Han, Y. M.; Qu, W. J.; Han, Z.; Zhang, R.; Wang, Y. X.; Chen, D.; Henze, D. K. Carbonaceous aerosols in China: top-down constraints on primary sources and estimation of secondary contribution. *Atmos. Chem. Phys.* **2012**, *12* (5), 2725−2746.
(51) Guo, S.; Hu, M.; Guo, Q. F.; Zhang, X.; Zheng, M.; Zheng, J.; Chang, C. C.; Schauer, J. J.; Zhang, R. Y. Primary Sources and Secondary Formation of Organic Aerosols in Beijing, China. *Environ. Sci. Technol.* **2012**, *46* (18), 9846−9853.
(52) Yang, F.; Kawamura, K.; Chen, J.; Ho, K.; Lee, S.; Gao, Y.; Cui, L.; Wang, T.; Fu, P. Q. Anthropogenic and biogenic organic comounds in summertime fine aerosols (PM2.5) in Beijing, China. *Atmos. Environ.* **2016**, *124*, 166−175.
(53) Kong, S. F.; Han, B.; Bai, Z. P.; Chen, L.; Shi, J. W.; Xu, Z. Receptor modeling of PM2.5, PM10 and TSP in different seasons and long-range transport analysis at a coastal site of Tianjin, China. *Sci. Total Environ.* **2010**, *408* (20), 4681−4694.
(54) Li, P. H.; Han, B.; Huo, J.; Lu, B.; Ding, X.; Chen, L.; Kong, S. F.; Bai, Z. P.; Wang, B. Characterization, Meteorological Influences and Source Identification of Carbonaceous Aerosols during the Autumn-winter Period in Tianjin, China. *Aerosol Air Qual. Res.* **2012**, *12* (2), 283−294.
(55) Li, X.; Zhang, Q.; Zhang, Y.; Zhang, L.; Wang, Y. X.; Zhang, Q. Q.; Li, M.; Zheng, Y. X.; Geng, G. N.; Wallington, T. J.; Han, W. J.; Shen, W.; He, K. B. Attribution of PM2.5 exposure in Beijing-Tianjin-Hebei region to emissions: implication to control strategies. *Sci. Bull.* **2017**, *62* (13), 957−964.
(56) Chow, J. C.; Watson, J. G.; Chen, L. W. A.; Chang, M. C. O.; Robinson, N. F.; Trimble, D.; Kohl, S. The IMPROVE-A temperature protocol for thermal/optical carbon analysis: maintaining consistency with a long-term database. *J. Air Waste Manage. Assoc.* **2007**, *57* (9), 1014−1023.

DOI: 10.1021/acsearthspacechem.9b00170
ACS Earth Space Chem. 2019, 3, 2339−2352

(57) Pavuluri, C. M.; Kawamura, K.; Aggarwal, S. G.; Swaminathan, T. Characteristics, seasonality and sources of carbonaceous and ionic components in the tropical aerosols from Indian region. *Atmos. Chem. Phys.* **2011**, *11* (15), 8215−8230.
(58) Kleindienst, T. E.; Lewandowski, M.; Offenberg, J. H.; Jaoui, M.; Edney, E. O. The formation of secondary organic aerosol from the isoprene plus OH reaction in the absence of NOx. *Atmos. Chem. Phys.* **2009**, *9* (17), 6541−6558.
(59) Wang, S.; Pavuluri, C. M.; Ren, L. J.; Fu, P. Q.; Zhang, Y. L.; Liu, C. Q. Implications for biomass/coal combustion emissions and secondary formation of carbonaceous aerosols in North China. *RSC Adv.* **2018**, *8* (66), 38108−38117.
(60) Zheng, B.; Tong, D.; Li, M.; Liu, F.; Hong, C. P.; Geng, G. N.; Li, H. Y.; Li, X.; Peng, L. Q.; Qi, J.; Yan, L.; Zhang, Y. X.; Zhao, H. Y.; Zheng, Y. X.; He, K. B.; Zhang, Q. Trends in China's anthropogenic emissions since 2010 as the consequence of clean air actions. *Atmos. Chem. Phys.* **2018**, *18* (19), 14095−14111.
(61) Mayol-Bracero, O. L.; Guyon, P.; Graham, B.; Roberts, G.; Andreae, M. O.; Decesari, S.; Facchini, M. C.; Fuzzi, S.; Artaxo, P. Water-soluble organic compounds in biomass burning aerosols over Amazonia - 2. Apportionment of the chemical composition and importance of the polyacidic fraction. *J. Geophys. Res.* **2002**, *107* (D20), 8091.
(62) Miyazaki, Y.; Kondo, Y.; Takegawa, N.; Komazaki, Y.; Fukuda, M.; Kawamura, K.; Mochida, M.; Okuzawa, K.; Weber, R. J. Time-resolved measurements of water-soluble organic carbon in Tokyo. *J. Geophys Res-Atmos* **2006**, *111* (D23), D23206.
(63) Aggarwal, S. G.; Kawamura, K. Carbonaceous and inorganic composition in long-range transported aerosols over northern Japan: Implication for aging of water-soluble organic fraction. *Atmos. Environ.* **2009**, *43* (16), 2532−2540.
(64) Simoneit, B. R. T. Biomass burning - A review of organic tracers for smoke from incomplete combustion. *Appl. Geochem.* **2002**, *17* (3), 129−162.
(65) Feng, T.; Zhao, S. Y.; Bei, N. F.; Wu, J. R.; Liu, S. X.; Li, X.; Liu, L.; Qian, Y.; Yang, Q. C.; Wang, Y. C.; Zhou, W. J.; Cao, J. J.; Li, G. H. Secondary organic aerosol enhanced by increasing atmospheric oxidizing capacity in Beijing-Tianjin-Hebei (BTH), China. *Atmos. Chem. Phys.* **2019**, *19* (11), 7429−7443.
(66) Fu, P.; Kawamura, K. Diurnal variations of polar organic tracers in summer forest aerosols: A case study of a Quercus and Picea mixed forest in Hokkaido, Japan. *Geochem. J.* **2011**, *45* (45), 297−308.
(67) Zhu, C.; Kawamura, K.; Fu, P. Seasonal variations of biogenic secondary organic aerosol tracers in Cape Hedo, Okinawa. *Atmos. Environ.* **2016**, *130*, 113−119.
(68) Claeys, M. Formation of secondary organic aerosols through photooxidation of isoprene. *Science* **2004**, *303* (5661), 1173−1176.
(69) Lin, Y. H.; Zhang, Z. F.; Docherty, K. S.; Zhang, H. F.; Budisulistiorini, S. H.; Rubitschun, C. L.; Shaw, S. L.; Knipping, E. M.; Edgerton, E. S.; Kleindienst, T. E.; Gold, A.; Surratt, J. D. Isoprene Epoxydiols as Precursors to Secondary Organic Aerosol Formation: Acid-Catalyzed Reactive Uptake Studies with Authentic Compounds. *Environ. Sci. Technol.* **2012**, *46* (1), 250−258.
(70) Riva, M.; Budisulistiorini, S. H.; Zhang, Z. F.; Gold, A.; Surratt, J. D. Chemical characterization of secondary organic aerosol constituents from isoprene ozonolysis in the presence of acidic aerosol. *Atmos. Environ.* **2016**, *130*, 5−13.
(71) Kroll, J. H.; Ng, N. L.; Murphy, S. M.; Flagan, R. C.; Seinfeld, J. H. Secondary organic aerosol formation from isoprene photo-oxidation. *Environ. Sci. Technol.* **2006**, *40* (6), 1869−1877.
(72) Surratt, J. D.; Murphy, S. M.; Kroll, J. H.; Ng, N. L.; Hildebrandt, L.; Sorooshian, A.; Szmigielski, R.; Vermeylen, R.; Maenhaut, W.; Claeys, M.; Flagan, R. C.; Seinfeld, J. H. Chemical composition of secondary organic aerosol formed from the photo-oxidation of isoprene. *J. Phys. Chem. A* **2006**, *110* (31), 9665−9690.
(73) Nguyen, T. B.; Bates, K. H.; Crounse, J. D.; Schwantes, R. H.; Zhang, X.; Kjaergaard, H. G.; Surratt, J. D.; Lin, P.; Laskin, A.; Seinfeld, J. H.; Wennberg, P. O. Mechanism of the hydroxyl radical oxidation of methacryloyl peroxynitrate (MPAN) and its pathway toward secondary organic aerosol formation in the atmosphere. *Phys. Chem. Chem. Phys.* **2015**, *17* (27), 17914−17926.
(74) Ciccioli, P.; Centritto, M.; Loreto, F. Biogenic volatile organic compound emissions from vegetation fires. *Plant, Cell Environ.* **2014**, *37* (8), 1810−1825.
(75) Haque, M. M.; Kawamura, K.; Kim, Y. Seasonal variations of biogenic secondary organic aerosol tracers in ambient aerosols from Alaska. *Atmos. Environ.* **2016**, *130*, 95−104.
(76) Schauer, J. J.; Kleeman, M. J.; Cass, G. R.; Simoneit, B. R. T. Measurement of emissions from air pollution sources. 2. C-1 through C-30 organic compounds from medium duty diesel trucks. *Environ. Sci. Technol.* **1999**, *33* (10), 1578−1587.
(77) Schauer, J. J.; Kleeman, M. J.; Cass, G. R.; Simoneit, B. R. T. Measurement of emissions from air pollution sources. 5. C-1-C-32 organic compounds from gasoline-powered motor vehicles. *Environ. Sci. Technol.* **2002**, *36* (6), 1169−1180.
(78) Oros, D. R.; Simoneit, B. R. T. Identification and emission factors of molecular tracers in organic aerosols from biomass burning Part 1. Temperate climate conifers. *Appl. Geochem.* **2001**, *16* (13), 1513−1544.
(79) Bahadur, R.; Uplinger, T.; Russell, L. M.; Sive, B. C.; Cliff, S. S.; Millet, D. B.; Goldstein, A.; Bates, T. S. Phenol groups in northeastern U.S. submicrometer aerosol particles produced from seawater sources. *Environ. Sci. Technol.* **2010**, *44* (7), 2542−2548.
(80) Fine, P. M.; Cass, G. R.; Simoneit, B. R. T. Chemical characterization of fine particle emissions from the fireplace combustion of wood types grown in the Midwestern and Western United States. *Environ. Eng. Sci.* **2004**, *21* (3), 387−409.

DOI: 10.1021/acsearthspacechem.9b00170
ACS Earth Space Chem. 2019, 3, 2339−2352